UNIVERSITAT DE BARCELONA

Final Degree Project

Biomedical Engineering Degree

IDENTIFYING THE NEURAL MECHANISMS OF PERCEPTUAL DECISION-MAKING IN A RAT AUDITORY TASK

Barcelona, 14th June 2021

Author: Emma Fernández i Miranda

Directors: Jaime de la Rocha and Genís Prat

Tutor: Agustín Gutiérrez Gálvez

Abstract

Perceptual decision-making involves accumulation of sensory information over time. The classical view indicates that sensory neurons first transform the physical stimulus into evidence, and then the decision making areas of the brain use this evidence to make a categorical choice. Here, we show that this process is not optimal. In general, rats do not equally weigh the stimulus and they underweight extreme stimuli values. These results indicate that there must be a non-linearity in the stimulus transformation into evidence or that the accumulation of evidence is not perfect.

To differentiate which are the underlying mechanisms that are causing these behaviours, we fitted an extended neurobiological model which was composed of a stimulus to evidence and a decision module. Using model comparison methods, we were able to identify that a non-linear stimulus to evidence transformation is relevant to explain the psychophysical kernels of the experimental task, but that time adaptation of the sensory neurons does not have an impact in this case. We also found that, at least for a subset of rats, the non-linear dynamics in the decision module explains the experimental data better than a linear perfect integration model.

Our work shows that model fitting is a powerful tool to investigate different brain mechanisms and that non-linear dynamics could be important not only during the accumulation of evidence but also during the stimulus to evidence transformation.

Keywords: Computational Neuroscience; Perceptual Decision Making; Neural Mechanisms; Model Fitting; Biomedical Engineering.

Acknowledgements

First of all, I would like to express my sincere gratitude to my supervisors. I am very thankful to Genís Prat, for his guidance and continuous support, and for the time he has invested in teaching me all the concepts necessary to develop this study. Without his help and suggestions, this project would not have been possible. I also wish to offer my sincere thanks to Jaime de la Rocha, for giving me the opportunity to work on such an interesting topic and for providing me with great mentorship throughout the development of the project.

I would like to extend my acknowledgement also to my tutor, Agustín Gutiérrez, for the help and advice he has given me.

In addition, I would like to thank my friends, who have made these years much more enjoyable and have helped me take my mind off the project when I most needed it. Finally, I would like to express my deepest gratitude to my parents and my two younger siblings, for always being by my side and for listening to my long chats about the project. I cannot imagine going through this process without them.

Contents

List of Figures

List of Tables

Acronyms

2AFC: Two-Alternative Forced Choice.

PI: Perfect Integrator.

DDMA: Drift Diffusion Model with Absorbing bounds.

DDMR: Drift Diffusion Model with Reflecting bounds.

DWM: Double-Well Model.

PK: Psychophysical Kernel.

AIC: Akaike Information Criterion.

IDIBAPS: Institut d'Investigacions Biomèdiques August Pi i Sunyer.

BSC: Barcelona Supercomputing Center.

SWOT: Strengths, Weaknesses, Opportunities and Threats.

PERT: Program Evaluation and Review Technique.

1 Introduction

There are times in life when the brain must respond to ambiguous stimuli and make a decision based on the integration of this information. During the COVID-19 pandemic, doctors, nurses, and even politicians, have had to make one of the most heart-breaking decisions anyone has to make: triage. Triage is fundamentally about balancing the consequences, and aims to provide the greatest amount of good for the maximum number of individuals. However, when intensive care units are full, morgues have run out of space, and there are not enough medical staff to care for all the patients, the decision of who is entitled to be treated and who has to go home with none or little medical help is very controversial.

Although it would be very interesting to know how these decisions are made, they are very difficult to study because they depend on multiple internal and external parameters which are hard to control experimentally. That is why we focus on simpler decisions involving only sensory stimuli (perceptual decision-making). For example, before crossing the street we have to see whether cars are moving or not and make a decision taking into account the visual information we have accumulated.

A common experiment used to study this type of decision-making is the random dot task, in which a cloud of dots moves and subjects must choose whether they move to the left or to the right. In this type of experiment, the experimenter can control the information and details that influence the final decisions, which makes it possible to attempt to deduce how the brain uses the stimuli to make decisions.

1.1 Perceptual decision-making

Perceptual decision-making is the process through which sensory information is gathered in order to make a choice. The classical view is that this process is done by decision areas which integrate the evidence provided by sensory areas until reaching a certain decision threshold.

Several experiments support this theory (Kiani et al. (2008), Roitman and Shadlen (2002), Britten et al. (1992), Shadlen and Newsome (2001), Nienborg and Cumming (2009)); they showed that the firing rate of sensory neurons (located in the medial

temporal cortex) was proportional to the stimulus strength that they received. It was also seen that the firing rate in the decision areas (located in the lateral intraparietal cortex) increased throughout the duration of the stimulus, which seemed to indicate the integration of the evidence provided by the sensory areas.

In these experiments, the evidence integration reaches a plateau after a certain value of the firing rate is reached which is independent of the stimulus strength presented, which indicates that there may be absorbing bounds while making the decision.

However, in more recent studies such as the one conducted by Brunton et al. (2013) or Waskom and Kiani (2018), it is seen that rats can integrate the evidence without the presence of these bounds. In other studies (Yates et al. (2017)) they show that sensory neurons can present time adaptation, which could explain the saturation of the evidence integration instead of the absorbing bounds in the evidence integration stage.

Thus far, several models have been proposed to understand this behaviour of how neurons integrate the stimulus information to make a categorical choice. These models range from phenomenological models which are based on a simple linear equation to more complex and biophysical models which are based on realistic neural circuits.

1.2 The drift-diffusion model with absorbing bounds

The drift-diffusion model with absorbing bounds (DDMA) is a phenomenological model that explains the choice and response time behaviour for a two-alternative forced-choice (2AFC) task by describing the temporal evolution of the decision variable. The decision variable represents the evidence of choosing one choice over the other at each time. The model accumulates evidence until one of the bounds is reached and the decision is made (fig. 1.1 a, center panel). If the bounds are not reached, the final decision of the model is the sign of the decision variable at the end of the trial.

The equation of the drift-diffusion model (eq. (1.1)) defines the temporal evolution of

the decision variable ($\frac{dx}{dt}$) and includes a drift rate (μ) which represents the evidence, a diffusion constant ($\sigma\xi(t)$) which represents the total noise (Gaussian stochastic process $\xi(t)$ with a standard deviation σ and mean 0) and a time constant (τ).

$$\tau\frac{dx}{dt} = \mu + \sigma\xi(t) \tag{1.1}$$

The total noise can be separated into internal or neural noise (σ_i) and external or stimulus fluctuations (σ_s). Thus the stimulus is a gaussian signal with mean μ and standard deviation σ ($S(t) = \mu + \sigma_s\xi(t)$). Since the internal noise is an intrinsic property of the brain, the only part of the noise which will be controlled during trials will be the environmental noise. Then, the drift-diffusion model can be defined as the motion of a particle (the decision variable) in a potential $\phi(x) = -\mu x$, obtaining the following expression:

$$\tau\frac{dx}{dt} = \frac{d\varphi(x)}{dx} + \sigma_i\xi_i(t) + \sigma_s\xi_s(t) \tag{1.2}$$

This is an stochastic differential equation that can be simulated using the euler method (eq. (1.3), fig. 1.1 a):

$$x(t+1) = x(t) - \frac{\Delta t}{\tau}\frac{d\varphi(x)}{dx} + \sqrt{\frac{\Delta t}{\tau}}(\sigma_i\xi_i(t) + \sigma_s\xi_s(t)) \tag{1.3}$$

where $\Delta t = \frac{\tau}{40}$.

The DDMA is widely used to study perceptual decision-making tasks. As explained before, several studies imply that the firing rate of the evidence integration areas reach a plateau which behaves as the absorbing bounds of the DDMA (Kiani et al. (2008)). The model can also explain other decision-making mechanisms if modified slightly, such as the bias (adding a parameter for an initial offset) (Gold et al. (2008), Urai et al. (2019), Mulder et al. (2012)), and confidence judgements or changes of mind (Kiani et al. (2014), Resulaj et al. (2009)).

Given the wide possibilities that the DDMA offers to explain experimental data, it is the most used to explain the behaviour of perceptual decisions, which is why it has been considered to be a canonical model in perceptual decision-making.

1.3 Canonical models of perceptual decision-making

Although the DDMA can explain a large body of the experimental data, it has been extended to explain the variability of behaviour across species and tasks. In this work we use three different versions of the canonical drift-diffusion model (Prat-Ortega et al. (2021)).

The standard **drift-diffusion model with absorbing bounds** (DDMA), in which the evidence is integrated until a certain bound is reached, when the decision is made.

The **drift-diffusion model with reflecting bounds** (DDMR), in which the evidence is integrated until the end of the stimulus, but a lower and upper boundary is set (it cannot integrate more than these boundaries).

The **perfect integrator model** (PI), in which evidence is integrated to the end of the stimulus and no boundaries are set.

In these models, when the evidence of right choice (or drift rate) is varied, the decision variable changes according to it. In figure 1.1 a, it can be seen that the perfect integrator model (fig. 1.1, left) integrates the stimulus without any bounds (i.e. the decision variable is simply the integral of the stimulus $S(t)$ plus the internal noise). In the DDMA (fig. 1.1, center), it can be seen that when the decision variable reaches a boundary, it does not change the decision variable anymore (it has reached a decision). In the DDMR (fig. 1.1, right), the decision variable changes after reaching the bound, but does not surpass them.

The accuracy (i.e. the probability that the sign of the decision variable at the end of the trial is equal to the sign of the mean evidence μ) depends on the two stimulus parameters (μ and σ_s). As μ increases the model becomes more deterministic and the accuracy increases (fig. 1.1 c). In contrast, as we increase the stimulus fluctuations (fig. 1.1 b), the variability of the decision variable increases which produces a decrease in the accuracy (fig. 1.1 d).

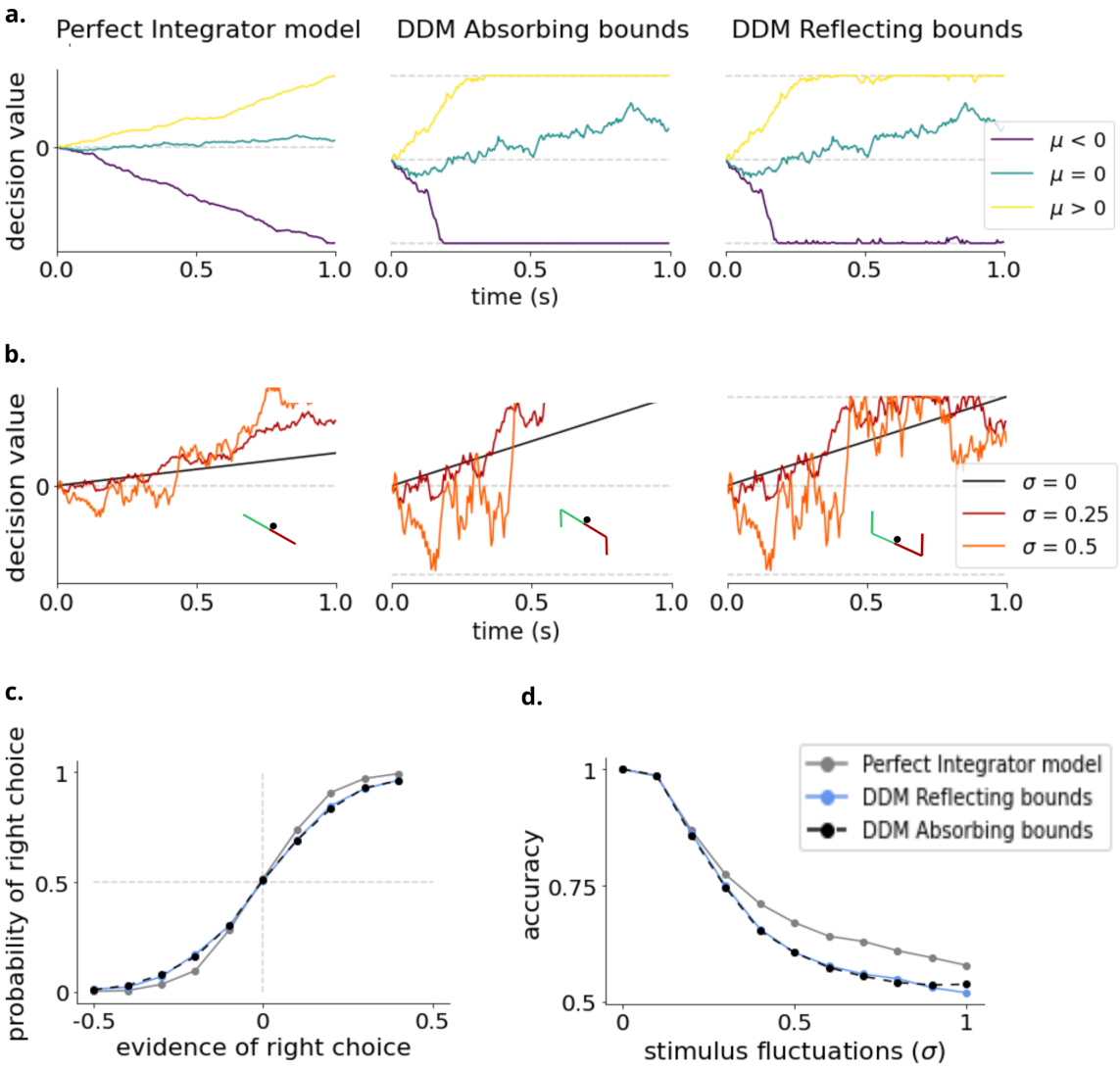

Figure 1.1 – Stimulus strength and noise effect on the drift-diffusion model.

a. Single traces for different evidence values ($\mu > 0$, $\mu = 0$ and $\mu < 0$). Left: perfect integrator, center: DDMR and right: DDMA. **b.** Simulation for different stimulus fluctuations σ = 0, σ = 0.25 and σ = 0.5. Left: perfect integrator, center: DDMR and right: DDMA. In the bottom right of the graphics the potential of each model. **c.** Psychometric curve (probability of right choice over μ) for the different models. **d.** Accuracy when changing the stimulus fluctuations (σ) for each model.

1.4 Psychophysical kernels

The **temporal psychophysical kernel** is an estimation of the impact of each frame on the final choice (fig. 1.2). The temporal PK for the perfect integrator model (fig. 1.2 a) is a flat line, since there are no bounds and thus the information is completely integrated. For the DDMA (fig. 1.2 b), the early frames have higher impact (we named

this effect primacy) than the late ones because when the decision variable reaches a boundary, the integration process ends. In contrast, in the DDMR (fig. 1.2 c) the late frames have a higher impact than the early ones (recency), because early fluctuations of the decision variable are not accumulated due to the reflecting boundaries. The **spatial psychophysical kernel** is a measure of the impact of each stimulus strength on the final decision. For each stimulus, a new vector with the frequency of each stimulus strength is calculated, and then logistic regression is applied to these new vectors and the final decisions (see Methods). The spatial PKs for the PI, DDMA and DDMR (fig. 1.2 d) are linear, which means that extreme levels of evidence have the most impact, while lower levels of evidence have less impact on the final decision (Waskom and Kiani (2018)).

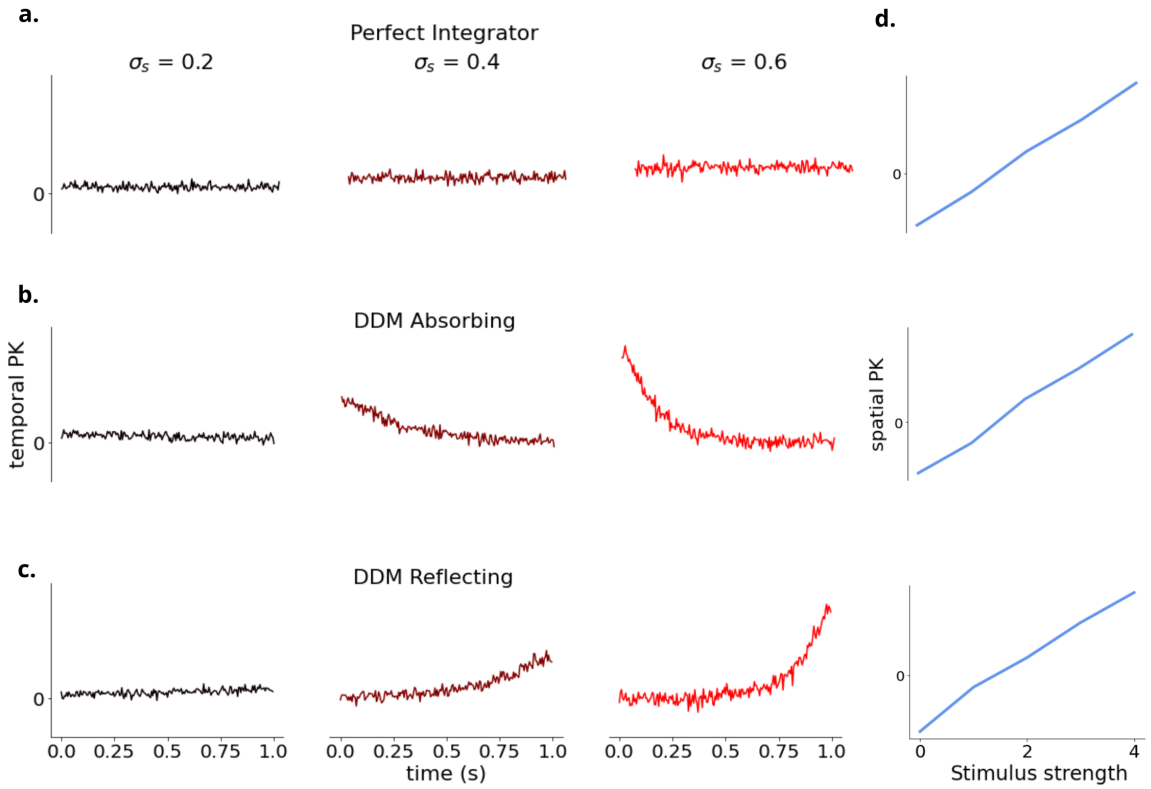

Figure 1.2 – Temporal and spatial psychophysical kernels of the DDM.

a. Temporal Psychophysical Kernel for the PI model, using $\sigma = 0.2$, 0.4 and 0.6. The temporal PK is flat. **b.** Temporal Psychophysical Kernel for the DDMA, using $\sigma = 0.2$, 0.4 and 0.6. As σ increases, there is a more pronounced pattern of primacy. **c.** Temporal Psychophysical Kernel for the DDMR using $\sigma = 0.2$, 0.4 and 0.6. As σ increases, there is a more pronounced pattern of recency. **d.** Spatial Psychophysical Kernel for the PI (top), DDM Absorbing (center) and DDM reflecting (bottom) models.

1.5 Biophysical models: the attractor network

Another approach to model 2AFC tasks are biophysical models. These models can reach different levels of description, and are based on cellular and network mechanisms that are observed by monitoring neural spiking activity during perceptual tasks. For perceptual decision-making, the standard biophysical model is made by two populations (which represent the possible choices) of excitatory neurons and one inhibitory population (fig. 1.3, Wang (2002)). Each neuron is modelled by a differential equation of its voltage. Before the stimulus presentation, the three populations are in a stable state of low activity. As soon as the stimulus is presented, the two excitatory populations increase their activity and they start to compete through the inhibitory population. The final stable state is one excitatory population with a high activity and the other with a low activity (Wang (2002)).

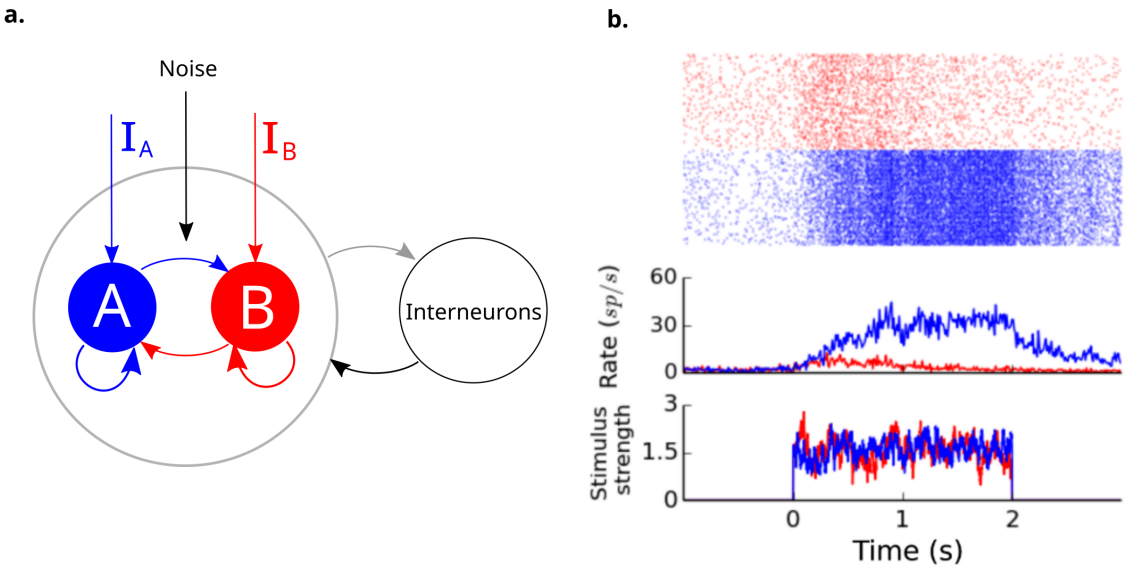

Figure 1.3 – Biophyiscal model proposed by Wang (2002).

a. Scheme of the biophysical model proposed by Wang (2002). There are two groups of excitatory neurons (A and B) with recurrent activity, which are selective to characteristics I_A or I_B of the stimuli. Both of these neural groups compete through an untuned population of inhibitory neurons. **b.** Single trial in the biophysical model. At the top it can be seen the raster plot of both populations of excitatory neurons. In the middle it can be seen how the two populations of excitatory neurons increase their firing rate when the stimulus is presented, until one of the populations wins. At the bottom, it can be seen the input that each population receives, which will be proportional to the stimulus evidence.[1]

[1] Extracted with author's permission from Prat Ortega (2019)

1.6 Double-well model

This two-choice neurobiological model can be reduced to a one-dimensional non-linear diffusion equation (Roxin and Ledberg (2008)), obtaining the double-well model (DWM). This way, a model which is made up of a large number of differential equations (one for each neuron), can be explained by a drift-diffusion process.

This equation explains the choice and response time behaviour for a two-alternative forced-choice task by describing the temporal evolution of the decision variable. It has the same equation as the drift-diffusion model, but the potential is different, it is defined by a quadratic expression (eq. (1.4)) resulting in a potential that has two attractors or wells (fig. 1.4 g).

$$\varphi(x) = -\mu x - c_2\frac{x^2}{2} + c_4\frac{x^4}{4} \tag{1.4}$$

where c_2 and c_4 are constants which will modulate the shape of the potential.

For this model, the accuracy decreases non-monotonically with the stimulus noise (fig. 1.4 f). A peak in the accuracy (flexible categorization) can be observed, which happens due to the phenomenon of transitions between the two wells ("changes of mind"). This peak can be explained by the shape of the DWM potential, since for a certain range of σ, the decision variable will be more likely to make correcting transitions (change from the wrong to the correct well) than to make error transitions. Time also affects this phenomenon since for lower stimulus durations there are no transitions (there is not enough time to change), and for higher stimulus duration there is more probability to make a transition to the correct well.

In figure 1.4 d, it can be seen that the temporal psychophysical kernel obtained by the DWM change its behaviour for different σ values. This is due to the phenomenon explained before of well transitions. For lower σ values it will show a primacy pattern, since there will not be as many well transitions, so the first frames will be the ones determining in which well the decision variable will fall and stay until reaching a decision. For higher σ values there is a recency pattern, since there will be too many transitions and thus the last frames will be the ones to determine which is the final

decision. For medium values of noise (which present flexible categorization), there will be a flatter pattern, so all the frames will have almost the same impact.

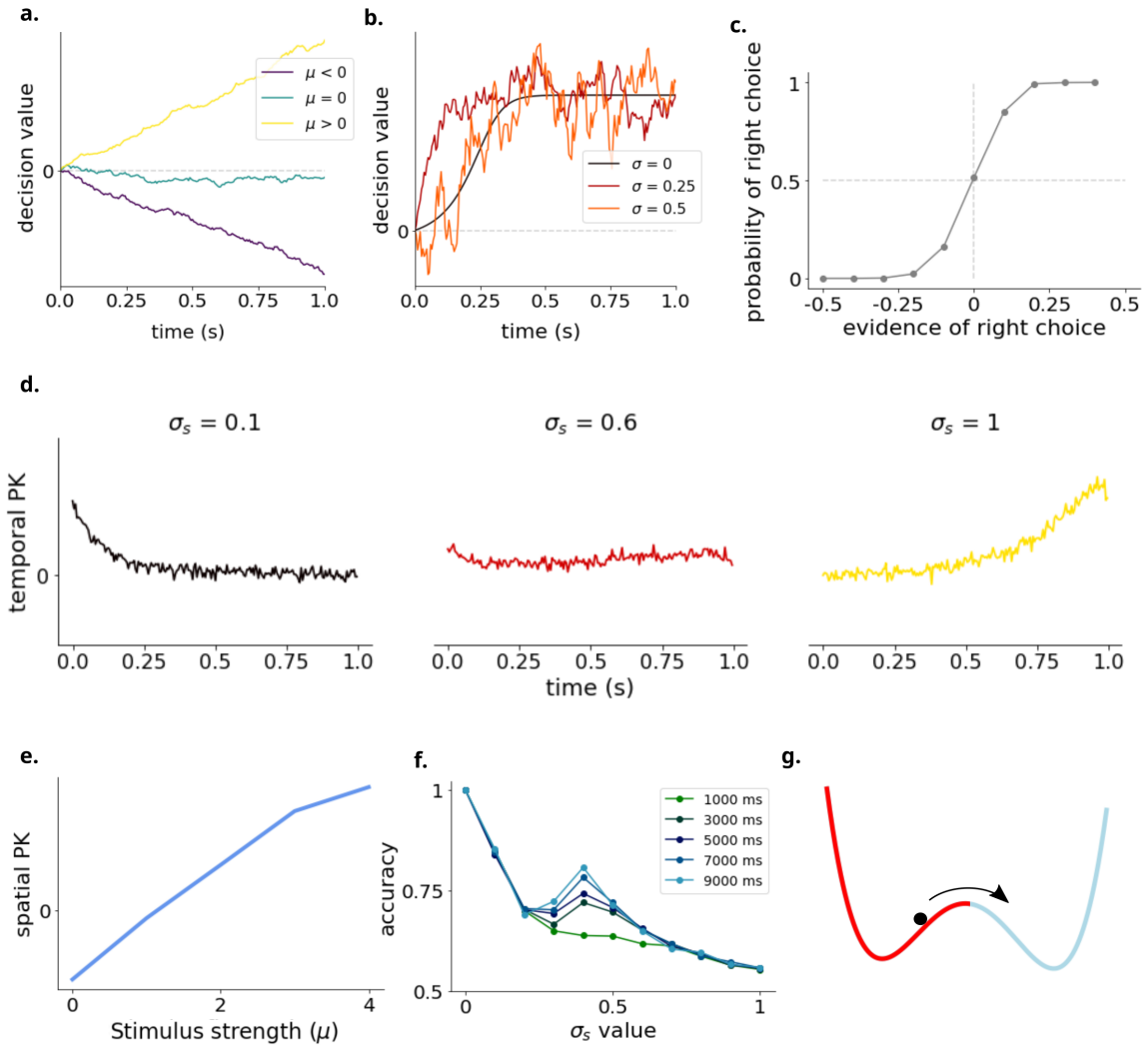

Figure 1.4 – Behaviour of the double-well model.

a. Single traces for different evidence values ($\mu > 0$, $\mu = 0$ and $\mu < 0$) for the double-well model. **b.** Simulation for different stimulus fluctuations $\sigma = 0$, $\sigma = 0.25$ and $\sigma = 0.5$ for the double-well model. **c.** Psychometric curve (probability of right choice over) for the DW model. **d.** Temporal psychophysical kernel, increasing σ to the right. For lower noise values, there is a primacy pattern and for higher noise values there is a recency pattern. **e.** Spatial psychophysical kernel for the DW model. **f.** Accuracy over σ for the DWM for different stimulus durations. **g.** DW potential, the black dot is the decision variable which can transition from one well to another.

As seen in figures 1.1 and 1.2, canonical models for perceptual decision-making can explain some of the mechanisms of experimental data and have a simpler equation

and behaviour than biophysical models, but they are not based on brain circuits, so they are not useful to understand how the brain is integrating the information. On the other hand, biophysical models can explain the connection between neurons and how they behave in order to reach a decision, but they are much more complicated and multi dimensional, which makes them difficult to fit.

The advantage of using the equation from Roxin and Ledberg (2008) is that the model can be used to fit experimental data, because the equation is one dimensional, but the behaviour is explained by the two attractor biophysical model which will gives us an insight on how neurons could be making the choices.

1.7 Objectives of this project

The main aim of this project is to understand how rats receive and integrate the information to make a categorical choice. To achieve this, the following consecutive minor objectives were set:

- Characterize the behaviour of 5 rats by analysing the data of a 2AFC task.
- Differentiate different mechanisms used to integrate the physical stimulus: the sensory stage and the decision stage.
- Develop and use a new model which explains the integration of sensory information, and is able to differentiate between the stimulus to evidence module and the decision module.
- Adapt an algorithm which is able to fit the double-well model so that it can fit the experimental data.

2 | Methods

2.1 Single traces

To simulate the diffusion equation (eq. (1.1)), we use the euler method (eq. (2.1)):

$$x(t+1) = x(t) - \Delta t \frac{d\varphi}{dx} + \sqrt{\Delta t}\xi(t)\sigma \tag{2.1}$$

with $\Delta t = \frac{\tau}{40}$.

In table 2.1, we have summarized the parameters used to plot the figures corresponding to model explaining (see Introduction).

	$\tau(ms)$	$dt(ms)$	μ	$T(ms)$	$bound$	σ	c_2	c_4
Figure 1.1 a	200	50	-0.5, 0, 0.5	1000	0.5	0.1	-	-
Figure 1.1 b	200	50	0.1	1000	0.5	0, 0.25, 0.5	-	-
Figure 1.1 c	200	50	-	1000	0.5	0.25	-	-
Figure 1.1 d	200	50	0.1	1000	0.5	-	-	-
Figure 1.2	200	50	0.1	1000	0.5	0.2, 0.4, 0.6	-	-
Figure 1.4 a	200	50	-0.5, 0, 0.5	1000	0.5	0.1	1	1
Figure 1.4 b	200	50	0.1	1000	0.5	0, 0.25, 0.5	1	1
Figure 1.4 c	200	50	-	1000	0.5	0.1	1	1
Figure 1.4 d and e	200	50	0.1	1000	0.5	0.1	1	1
Figure 1.4 f	200	50	0.1	1000, 3000, 5000, 7000, 9000	0.5	-	1	1

Table 2.1 – Parameters used to plot the figures from chapter 1.

2.2 Psychometric curves

The psychometric curves are the probability that the subject chooses the right choice plotted against the stimulus strength. To compute the probability to choose the right choice, trials are grouped by their stimulus strength value, which is calculated by making the mean of all stimulus frame values.
Then, for each stimulus strength, the percentage of right choices over left choices is computed, obtaining the percentage of times that the subject has chosen right throughout all the experiment for a certain stimulus value.

The confidence intervals are computed using the Wald method (eq. (2.2)) for a binomial distribution, considering that the level of confidence is 95%.

$$CI = \hat{p} \pm z\sqrt{\frac{\hat{p}(1-\hat{p})}{n}} \tag{2.2}$$

where $\hat{p}$ is the proportion of success and n the number of trials. z is the $1-\frac{1}{2}\alpha$ quantile of a standard normal distribution and α is the error rate. For a 95% confidence, α is 0.05, so $1-\frac{1}{2}\alpha = 0.975$ and therefore $z = 1.96$.

2.3 Psychophysical kernels

As explained in the previous chapter, the temporal psychophysical kernel gives us an estimation of the impact that each stimulus frame has on the final decision, while the spatial psychophysical kernel explains the impact of each stimulus strength on the final choice. Both temporal and spatial psychophysical kernels are the weights of a logistic regression model trained to predict the choices.

To compute the **temporal psychophysical kernel**, we trained the logistic regression model to predict rats' or models' choices given the stimulus. Thus each weight (w_i) is an estimation of the impact of a certain frame i:

$$\log(\frac{P_R}{1-P_R}) = \sum_{i=1}^{N_b} w_i s_i n_i \tag{2.3}$$

where P_R is the probability that the subject chooses the right choice, N_b the number of frames of each stimulus, s_i is the value of the stimulus at a certain frame i and n_i the number of the stimulus frame. To fit the logistic regression model, we use maximum likelihood estimation.

The **spatial psychophysical kernel** is a method to estimate the impact of each stimulus strength on the final choice. First we compute an histogram of each stimulus, we bin the stimulus space in bins of $\Delta X = 0.1$ and we count how many frames belong to each bin.
For example, if we have a stimulus which is:

$$[0.01, 0.13, 0.29, -0.19, 0.15, 0.05, -0.12, 0.07, 0.24, 0.12]$$

and we know that the stimulus values range from -1 to 1, we will obtain a new vector with 20 components: the first will be the number of times that the stimulus frame has a value between -1 and -0.9, then the second will be the amount of times that the stimulus frame has a value between -0.9 and -0.8, and we repeat this until reaching the 20^{th} component, which will be the number of times that the stimulus frame has a value from 0.9 to 1 appears during the trial. The new vector (transformed stimulus) that is obtained is:

$$[0, 0, 0, 0, 0, 0, 0, 0, 2, 0, 3, 3, 2, 0, 0, 0, 0, 0, 0, 0]$$

Then, logistic regression is applied using these new vectors and the final choices. This is done by changing n_i which is the frequency of stimulus strength in a trial and w_i, which is the weight that each stimulus strength has on the final decision in equation 2.3.
The confidence intervals in both cases are computed based on a standard normal distribution using student's T test.

2.4 Model fitting

The fitting of each model to the psychophysical data is performed using maximum likelihood estimation. If we consider that each rat has N trials and N responses, and

that trials are independent, the likelihood of this data given a certain model is:

$$l = \prod_{i=0}^{N} p(r_i = d_i \mid \theta, S_i) \tag{2.4}$$

where θ are the parameters of the model and $p(r_i = d_i \mid \theta, S_i)$ is the probability of the model predicting the same decision as the subject for the i^{th} trial. By doing this, we are maximizing the chance that the model makes choices equal to the original data decisions.

The logarithm of the likelihood is maximized instead of the likelihood to avoid computational problems (the sum of the log-likelihoods is performed instead of the multiplications of the likelihoods):

$$\log(l) = \sum_{i=0}^{N} \log(p(r_i = d_i \mid \theta, S_i)) \tag{2.5}$$

To maximize the log-likelihood, we use a gradient descent algorithm adapted from Yartsev et al. (2018).

Since the code has to compute the probability of right for each of the trials, it is very expensive computationally. That is why during this stage of the project, the cluster of the Barcelona Supercomputing Centre was used. This gave us access to a high number of processors (approximately 10000), which made the code run faster and allowed us to have the results of 1 fitting for all subjects in approximately 12 hours. Without the use of this resource, it would not have been possible to do this project.

2.5 Probability of right of each trial

We compute the probability of right for each trial using the distribution of the decision variable at the end of the stimulus $p(X, T)$, where T is the stimulus duration and X the decision variable. The probability of right is the positive area of this distribution.

The decision variable follows the equation 1.1 seen in the previous section. Using the equation 2.1 we can determine that the distribution of the decision variable at time $t+1$

is given by:

$$p(X,\, t+1) = N\left(X(t) - \frac{d\varphi}{dX}\Delta t,\, \sqrt{\Delta t}\sigma\right) \tag{2.6}$$

which depends on the previous position of the decision variable. To compute the distribution of the decision variable throughout the duration of the trial, we use a Markov transition matrix (or forward matrix) (fig. 2.1 center).

To compute the forward matrix, we discretize the decision variable space in $2N_b + 1$ bins which have a width of ΔX. Then, we compute the bin centers: $v_i = (i - N_b)\Delta X$ with $i = 0$ to $2N_b$, and the bounds of the bins: $\alpha_i = i\Delta x - N_b\Delta X - \frac{\Delta X}{2}$ with $i = 0$ to $2N_b + 2$. The area of equation 2.6 that is inside a certain bin j will be the probability that a transition is made from bin i to bin j.

This matrix contains the information of the probability of the decision variable at the immediate next time step (temporal evolution of the decision variable). So it explains the probability to make a transition from a value to another for a time step Δt.

If the decision variable at a certain time is multiplied once by the forward matrix, the result is the distribution of the decision variable at the next time step (fig. 2.1).

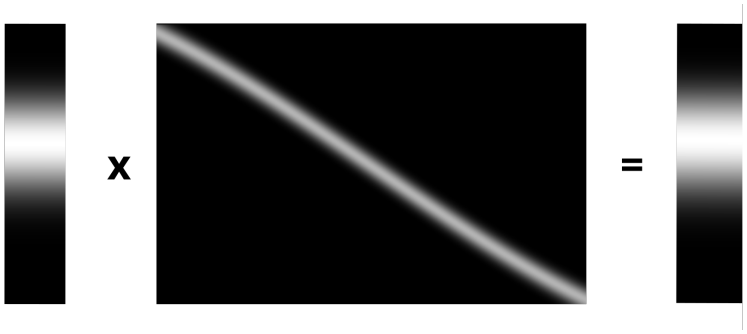

Figure 2.1 – Distribution of the decision variable at $t + 1$ obtained by multiplying the distribution at t and the forward matrix.

Knowing this, we can use the forward matrix to compute the distribution of the decision variable at a certain time (T_i) multiplying initial decision variable value by the forward matrix elevated to the number of time steps to reach T_i (fig. 2.2 b).

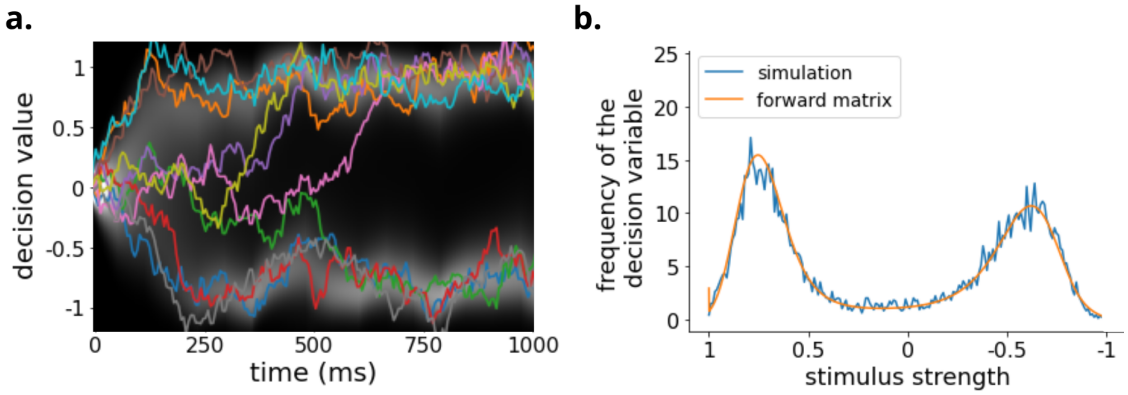

Figure 2.2 – Distribution of the decision variable obtained using the forward matrix.

a. Distribution of the decision variable throughout time (in white) and single trials (colored lines). **b.** Distribution of the decision variable at a $t = 400ms$ obtained by simulations (blue) and obtained by multiplying the initial decision variable value by the forward matrix elevated to 400 time steps.

2.6 Model comparison

To quantify the importance of each model parameter to fit the data, we fitted the data with and without the parameter. We quantify the importance of each parameter by subtracting the Akaike Information Criterion (AIC) of the full model and the model without the parameter. We use the AIC because it takes into account the number of parameters:

$$AIC = 2K - 2\ln(l) \tag{2.7}$$

where K is the number of parameters and l the likelihood of the model. If the difference between the AIC value of two models compared is greater than 10, we consider that there is strong evidence that the parameter is important to explain the data (Shen and Ma (2018)).

2.7 Checking that the fits are reliable

To check the probability of right is correctly computed, we compared the probability of right for each trial computed using the forward matrix (PR forward matrix), and by making simulations directly using the equation of the model (eq. (2.1)), PR

simulations). The linearity of this plot (fig. 2.3) indicates that the forward matrix is able to compute correctly the probability of right of single trials.

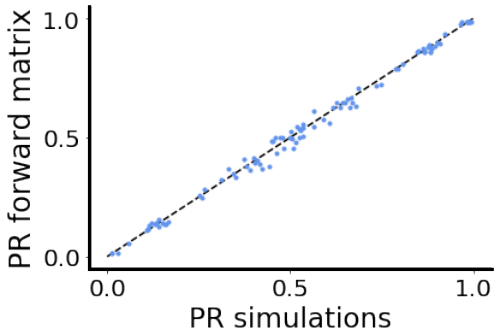

Figure 2.3 – **Reliability of the fit.**

Probability of right obtained using the forward matrix (y-axis) compared to the probability of right using simulations of the equation of the model (x-axis).

2.8 Availability of the code

The code created throughout the project can be found at: https://github.com/emmafdz/FinalDegreeProject, and has been done in collaboration with Genís Prat, postdoctoral researcher at IDIBAPS (Institut d'Investigacions Biomèdiques August Pi i Sunyer).

3 | Results

3.1 Experimental data

In order to identify the mechanisms underlying the decision-making process, we used data from an auditory 2AFC task. The task consisted of free field stereo amplitude-modulated noises $\eta(t)$ with a maximum intensity of 70dB. The stimuli were drawn from a beta distribution with mean e_K (stimulus strength) and a standard deviation of σ_K (stimulus fluctuations) which determined the amplitude of the left and right envelopes at each trial (eq. (3.1)):

$$\textbf{Lateralized evidence} \begin{cases} a_L^k(t) = 0.5(1 - e_K(t)) \\ a_L^k(t) = 0.5(1 + e_K(t)) \end{cases} \tag{3.1}$$

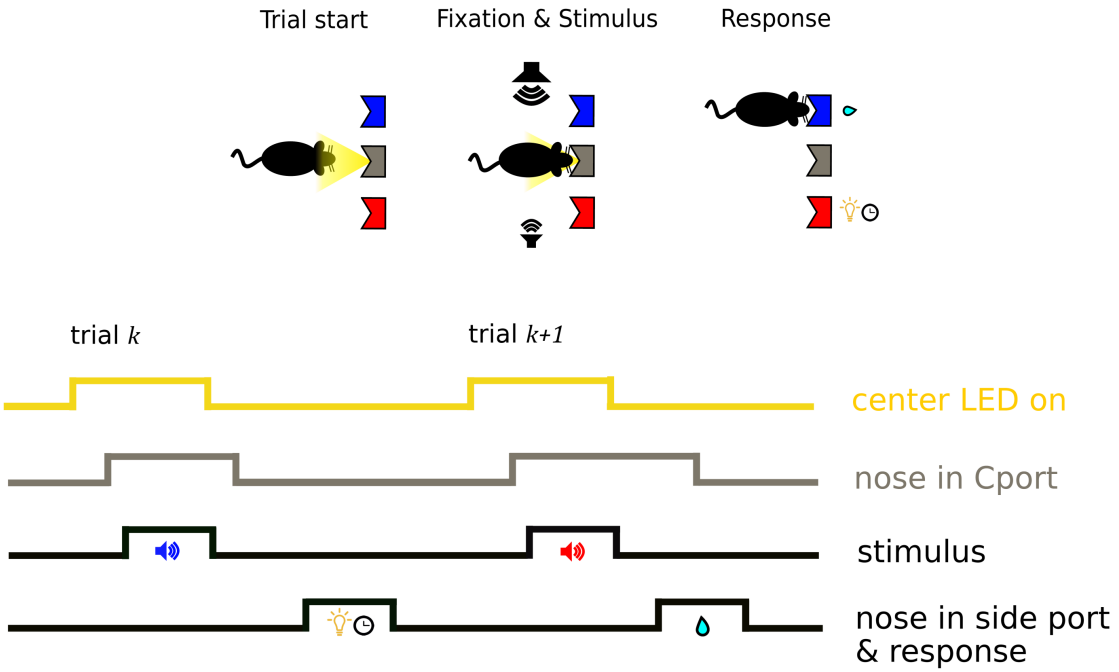

Figure 3.1 – Rats auditory discrimination task.

The trial starts when the rat pokes in the center port. First, the LED light in the center port is lit, then the rat pokes in the center port and after a fixation period of 300 ms, the auditory stimulus with evidence to the left or to the right is presented. Once the stimulus is off, rats can find the reward on the port associated with the loudest sound during the stimulus presentation and obtain a reward (water) or the wrong port, where they are punished with a light plus a 5 second timeout.

The animals had to integrate the stimulus evidence coming from the left and right speakers in order to decide from which of the two speakers the sound was louder and then seek the reward in the correct port (fig. 3.1).

Five rats participated in the experiment with different stimulus duration: we used 0.5 seconds stimuli for rats 24 and 36, 1 second stimuli for rat 35 and both duration for rats 25 and 37. In each trial, the parameters of the generative stimulus distribution (σ_K and e_K) were randomly chosen from one of the possible values: σ_k = 0.0, 0.1129, 0.255, 0.576 and 0.8 and e_K = -1.0, -0.5, -0.15, 0.0, 0.15, 0.5 and 1.0.

In this project, we are not interested in how the rats learned this task, thus we excluded all the data from training stages. Also, trials where the animals broke fixation were classified as invalid and were excluded from the analysis.

Since the behaviour of the rats when given different stimulus durations varied significantly, they were studied separately for each stimulus length, so in total we will have 7 different subjects:

- Rat 24 with a stimulus duration of 0.5 seconds.
- Rat 25 with a stimulus duration of 0.5 seconds.
- Rat 25 with a stimulus duration of 1 second.
- Rat 35 with a stimulus duration of 1 second.
- Rat 36 with a stimulus duration of 0.5 seconds.
- Rat 37 with a stimulus duration of 0.5 seconds.
- Rat 37 with a stimulus duration of 1 second.

3.2 Experimental results

3.2.1 Psychometric curves

The psychometric curve shows the percentage of right choices for each stimulus mean (fig. 3.2). And it helps us know if the rats have learned the task correctly (i.e.

they will make mostly correct choices when the evidence values are extreme).

For **rat 24** (with stimulus duration of 0.5 seconds), **rat 35** (with stimulus duration of 1 second), **rat 36** (with stimulus duration of 0.5 seconds) and **rat 25** (with stimulus duration of 1 second) the psychometric curve has the shape of a sigmoid (a cumulative Gaussian function), and for stimulus strength 0 (which means no evidence of left or right is given) there is a 50% rate of right choices. As expected from a trained animal the accuracy increases with the stimulus strength.

For **rat 25** (with stimulus duration of 0.5 seconds), **rat 37** (with stimulus duration of 0.5 and 1 seconds) the psychometric curve is biased. There is a shift to the right, which means that when the stimulus strength is 0, the rat makes less than 50% of right choices.

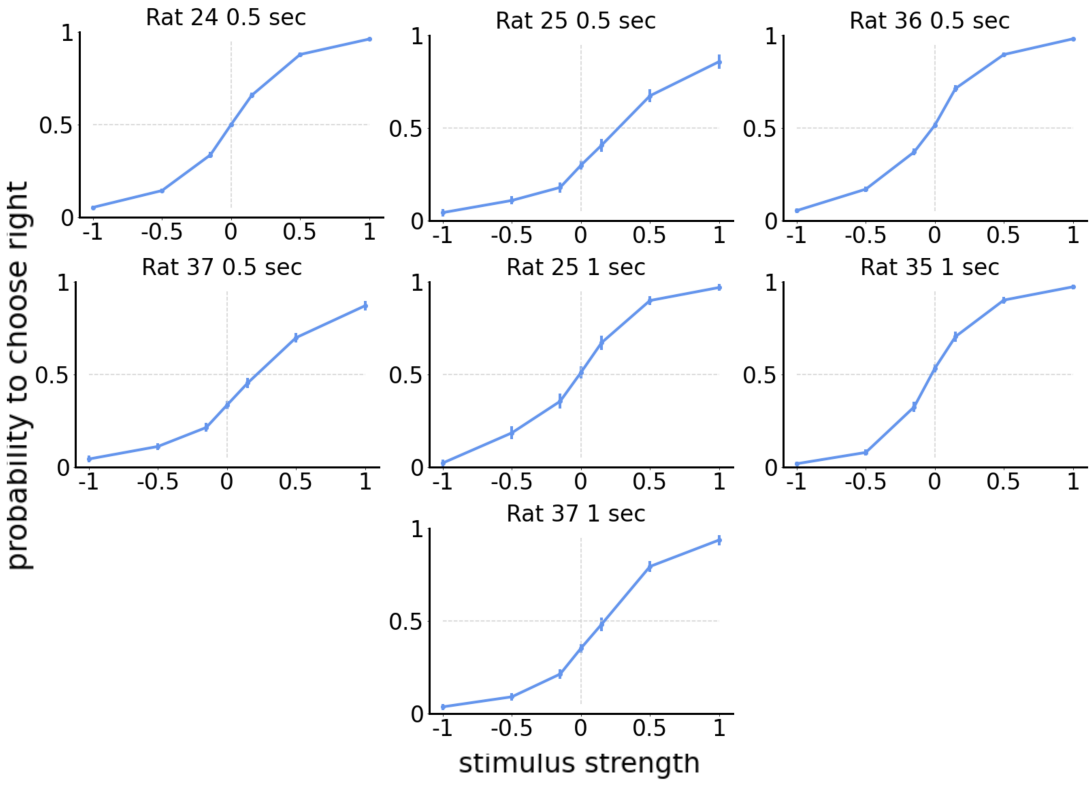

Figure 3.2 – Psychometric curves obtained from the experimental data.

The behaviour of the rats which have a shift in the psychometric curve can be explained by different bias mechanisms that could be added to the model, but this is out of the

scope of this project. In future applications, different biases should be added in order to see where these shifts in the psychometric curve originated.

3.2.2 Temporal psychophysical kernels

Having shown that rats have learned the task, we studied the impact that each frame has on the final decision. The psychophysical kernel of the canonical models are either primacy (the first frames have more impact on the final decision), flat (all the frames have the same impact) or recency (the last frames have stronger impact on the final choice). The double-well model can account for primacy, recency and a mix of both named flexible categorization (Prat-Ortega et al. (2021)).

In the experimental results (fig. 3.3), we found that some of the rats did not have a recency or primacy pattern, but rather a mix of both of these behaviours and there were some of the rats which present a temporal PK compatible with the flexible categorization regime of a double-well model (i.e. rat 24).

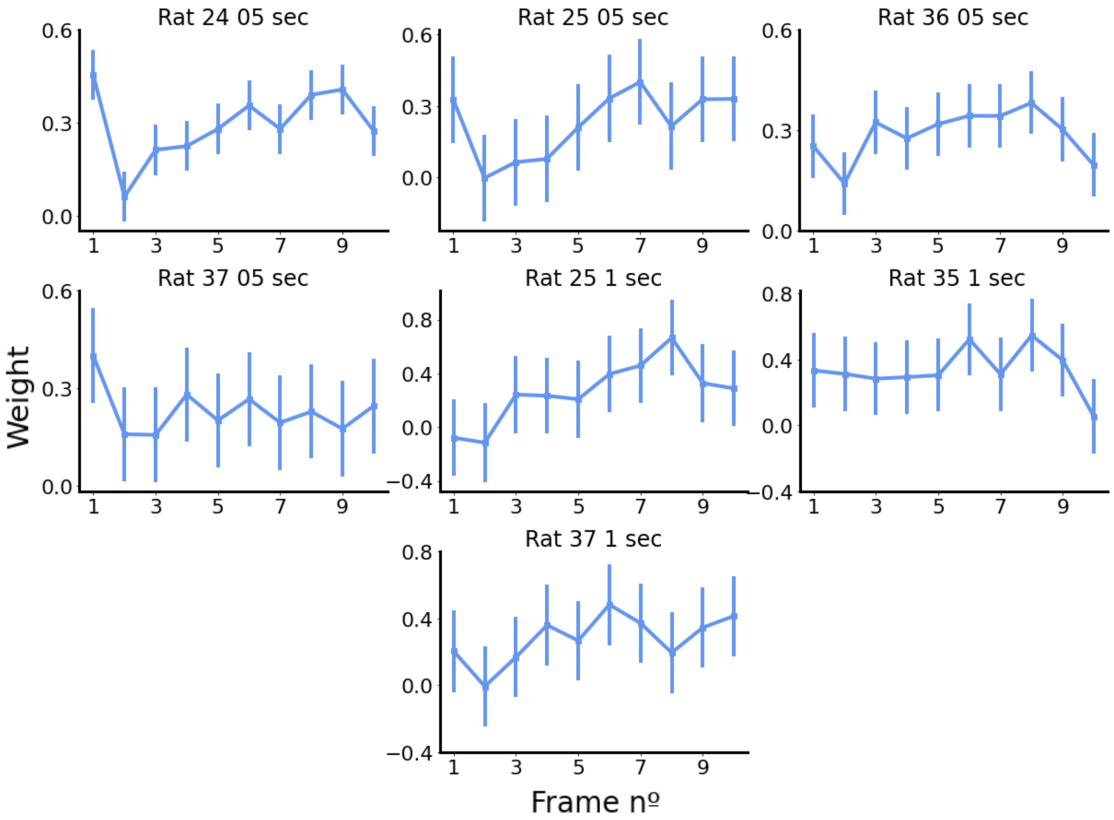

Figure 3.3 – Temporal Psychophysical kernels obtained from the experimental data.

For **rat 24** and **25** (with 0.5 seconds of stimulus duration), the first frame had a strong impact on the decision, the second frame had almost no impact but then the weight increased until reaching a similar impact than the first frame. This resembles the effect of flexible categorization.

For **rat 36** (with 0.5 seconds of stimulus duration) and **rat 35** (with 1 second of stimulus duration) it has a flatter pattern, and the frames which had the highest weight when deciding the final choice are the ones in the middle.

For **rat 37** (with 0.5 seconds of stimulus duration), the temporal PK was primacy whereas for **rats 25** and **37** (with 1 second of stimulus duration) the kernel was recency.

Since the temporal psychophysical kernels of the rats are heterogeneous, it is expected each rat is explained by a different model or by the same model with different parameters. That is why during the fitting stage of the project, it was decided that the data for each rat would be fitted separately.

3.2.3 Spatial psychophysical kernels

The spatial psychophysical kernel is a measure of the impact that each stimulus strength has on the final decision. If the integration of the stimulus is perfect, the spatial PK is linear, and a frame with stimulus evidence $2X$ has two times the impact of a frame with evidence X. However, this was not the case for our experiment (fig. 3.4), since rats tended to underestimate extreme values of evidence.

This effect can be caused by a non-linearity either on the stimulus to evidence or the decision module, but we cannot differentiate which is the module that has this non-linearity just by looking at these results.

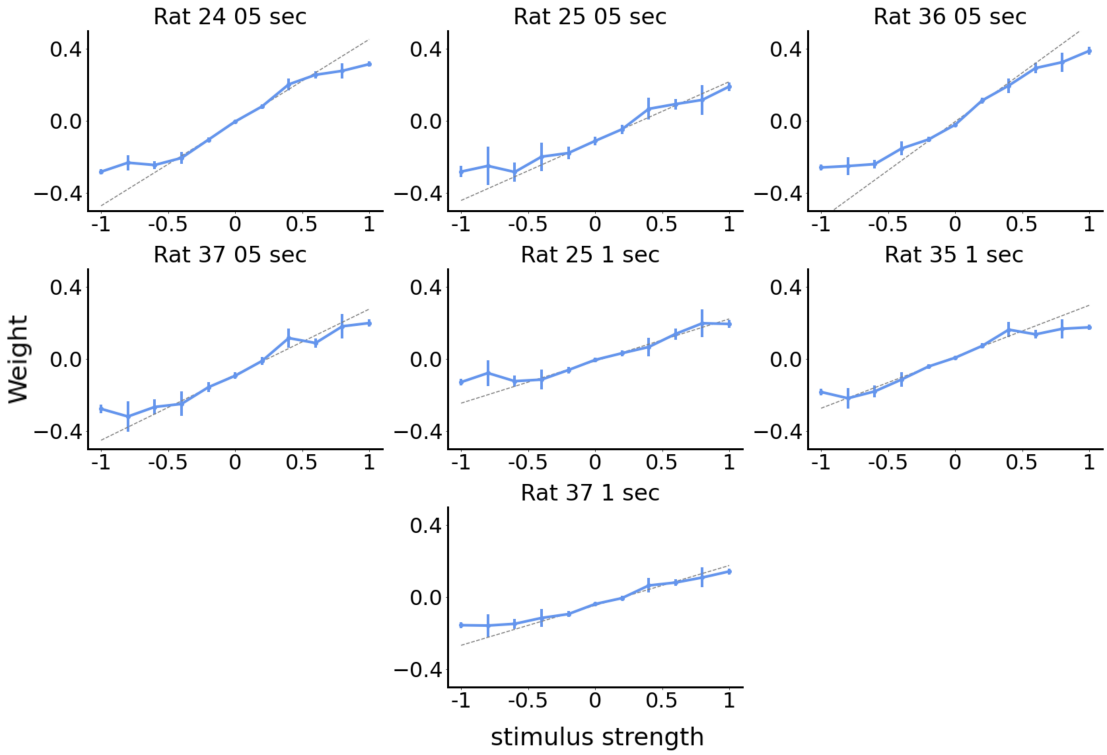

Figure 3.4 – **Spatial psychophysical kernels obtained from the experimental data.**

3.3 Extended attractor model

Once we characterized the behaviour of rats in our auditory discrimination task, we next investigated the possible mechanisms that can account for this behaviour. First, we did a qualitative comparison of the existing models and our behaviour results. We realized that the temporal and spatial psychophysical kernels cannot be explained by canonical models nor the double-well model alone, so other mechanisms would have to be studied. Thus we decided to build and fit an extended attractor model to quantify the importance of each possible mechanism. This model had different parameters that were based on the following empirical observation of the neural circuits:

Non-linear stimulus to evidence transformation: As explained in the introduction, the process of perceptual decision-making can be divided in two steps. First, the sensory module transforms the physical stimulus into evidence supporting one of the two choices, and the decision module which accumulates the evidence to maximize the accuracy (fig. 3.5).

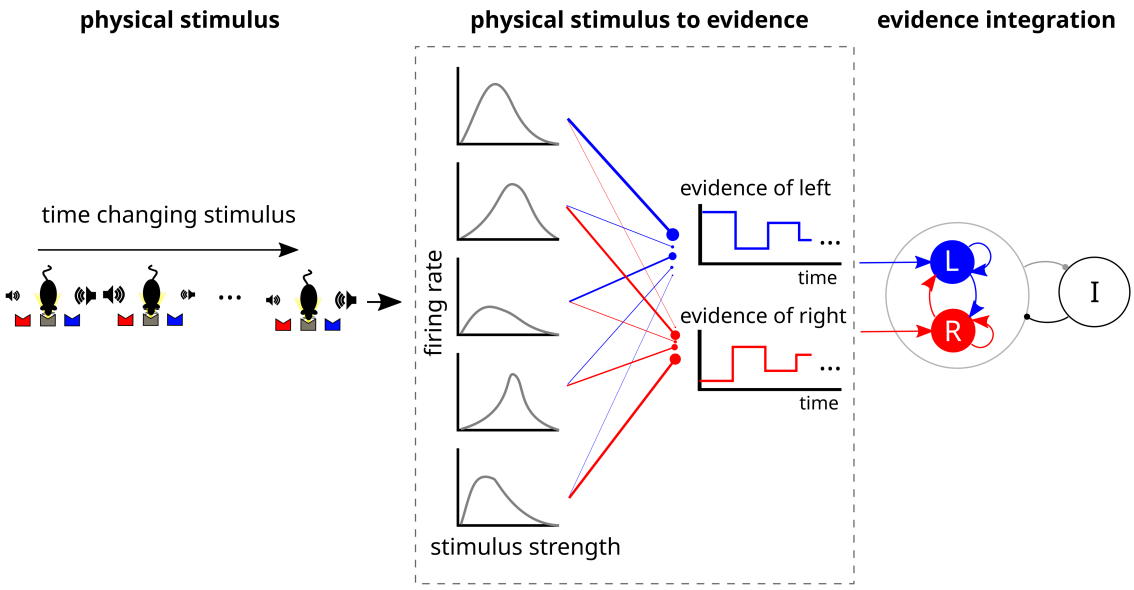

Figure 3.5 – Classical view of perceptual decision-making.

At the **left**, the physical stimulus, which will change through time. At the **center**, the physical stimulus to evidence step, at the left the tuning curves of the sensory neurons, which will transform the stimulus into evidence depending on their firing rate. At the **right**, the evidence integration module, where two populations of excitatory neurons will compete through an inhibitory untuned population to reach a decision.

In the sensory step, the neurons from sensory areas represent the stimulus information with its firing rate. For instance there are neurons with a high firing for right evidence and low firing rate for left evidence. The response of these neurons has been assessed in several studies obtaining the average firing rate of the neuron for each grade of the stimulus (tuning curves) (fig. 3.5 center, Butts and Goldman (2006)). In the case of the experimental task used in this project, neurons are selective to a certain auditory frequency coming from either the left or the right side. Then, these neurons (fig. 3.5, center) transmit the information to the decision circuit (fig. 3.5, right). A possible model for this circuit is the biophysical attractor network explained in the introduction.

Time adaptation of the sensory neurons: It also has to be taken into account that these neurons can adapt to the stimulus throughout time (Yates et al. (2017)). This means that for the same stimulus value, their firing rate decreases over time. For example, when we enter a new room and a certain smell is detected, the sensory

neurons at first send a strong signal of this smell, but after some time the smell does not seem as strong because neurons have gotten “used to” receiving this stimulus.

Taking into account these biophysical constraints we built and fitted a model with two modules: the stimulus to evidence module and the decision module. In the stimulus to evidence module, the physical stimulus was transformed to evidence and then the decision module accumulated this evidence to make the final decision.

A logistic transformation (fig. 3.6, eq. (3.2)) was chosen for the stimulus to evidence transformation module. From previous studies (Waskom and Kiani (2018), Drugowitsch et al. (2016)) and in our experimental results, the spatial psychophysical kernels had a logistic pattern, which could be explained by this type of transformation. Also, a parameter which changes the slope for each frame was added to mimic the temporal adaptation of the sensory neurons seen in previous studies (Yates et al. (2017)).

$$\mu_j = \frac{2}{A}\left(\frac{1}{e^{\beta+\beta_t*(t-1))*s}} - \frac{1}{2}\right) \tag{3.2}$$

where μ_j is the evidence, $\frac{1}{A}$ is the saturation value of the logistic curve, $\frac{1}{\beta}$ is the slope, β_t is the parameter that will change the slope throughout time and s is the physical stimulus.

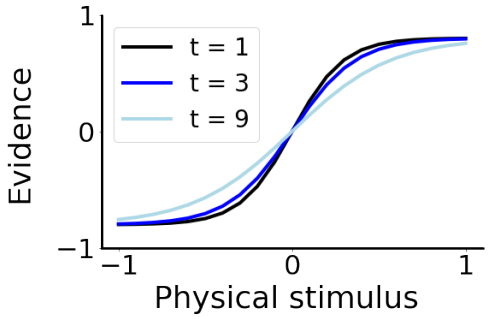

Figure 3.6 – Logistic transformation of the stimulus, which changes its slope for each frame.

In the decision module we used the double-well model (Roxin and Ledberg (2008)), which is the one-dimensional version of the two attractor model by Wang (2002).

3.4 How to identify the mechanisms underlying the behaviour of the psychophysical kernels

To illustrate that by fitting the model we can differentiate between mechanisms that generate similar psychophysical results, we generate data with different models and we recover the original parameters.

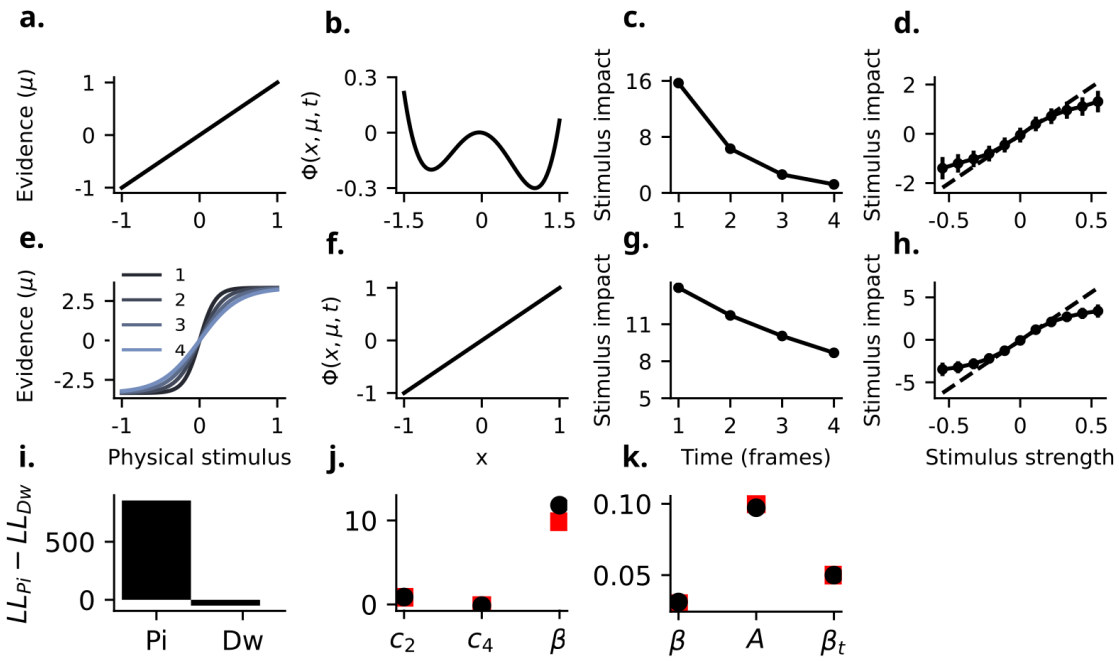

Figure 3.7 – Temporal and Spatial Psychophysical Kernels obtained with only non-linear mechanisms either in the decision step or in the stimulus to evidence step.

a. Linear stimulus to evidence function. **b.** The decision module (double-well potential) for different values of the evidence μ. **c.** Temporal Psychophysical Kernel generated by a non-linear decision module showing a primacy pattern. **d.** Spatial Psychophysical kernel generated by a non-linear decision module which underweights extreme stimulus strengths. **e.** Logistic stimulus to evidence transformation with time adaptation, each line is the transformation function at a certain frame. **f.** Linear potential (perfect integrator) of the decision module for different values of evidence μ. **g.** Temporal Psychophysical Kernel generated by a logistic stimulus to evidence module showing a primacy pattern. **h.** Spatial Psychophysical kernel generated by a logistic stimulus to evidence module which underweights extreme stimulus strengths. **i.** We compare the likelihood of the fittings of two synthetic data sets. **j** and **k.** The parameters are recovered in both fits using 7000 trials.

For instance, the first row (fig. 3.7 a, b, c and d) corresponds to synthetic data generated with a linear stimulus to evidence module (which cannot cause the shape of the spatial psychophysical kernel) combined with a double-well model for the decision

module. In this case, the temporal psychophysical kernel obtained is primacy pattern and the spatial psychophysical kernel is not linear.

On the second row (fig. 3.7 e, f, g and h) the synthetic data was generated with a logistic stimulus to evidence module, which changes its slope in each frame (due to time adaptation of the sensory neurons) and a linear decision module (a perfect integrator model) which cannot cause the non-linear spatial psychophysical kernel by its own. The temporal psychophysical kernel also shows a primacy pattern, and we also obtain a spatial psychophysical kernel very similar to the one obtained with the first model.

Qualitatively, the temporal and spatial psychophysical kernels look very much alike (fig. 3.7 c, d and g, h), so it is not possible to differentiate qualitatively if this primacy on the temporal psychophysical kernels and this non-linear pattern on the spatial psychophysical kernels are generated by non-linearities on the stimulus to evidence module or the decision module.

In order to identify which model was used to create each data set, we fitted both models by maximum likelihood estimation (see Methods) to the data created with both models. Then we can compare the log-likelihood of the fittings (fig. 3.7 i).

First, the data created with the model with PI (non-linear stimulus to evidence module and linear decision module) was fitted using both models: the one with PI and the one with DW (model with linear stimulus to evidence module and non-linear decision module). When comparing the log-likelihood of both of these fittings, we found that the log-likelihood of the fitting with the model with PI was much higher (there was a difference in the log-likelihood of both fittings of more than 500, fig. 3.7 i). If we use the formula (eq. (3.3)) we can obtain the probability that the model i minimizes the information loss.

$$exp\left(\frac{AIC_{min} - AIC_i}{2}\right) \tag{3.3}$$

In this case, the AIC difference was 500 obtaining that the model with DW was 2.66919e-109 times probable to obtain a fit as good as the model with PI. This suggests that there is strong evidence that this data was created by the model with PI.

Then, the data created with the model with DW was fitted using both models. Again we found strong evidence that this data was created with the DW model, ($LL = -50$, fig. 3.7 i). Using equation 3.3, it was obtained that the model with PI was 1.3887944e-11 times probable to obtain a result as good as the model with DW. By analysing these results, it has been concluded that it is possible to differentiate if the data is created with a non-linear stimulus to evidence module or a non-linear decision module by fitting the original data and comparing the log-likelihoods of the fittings.

The reason why this is only detectable by comparing the log-likelihoods, but it is not detected qualitatively in the psychophysical kernels, is that when computing both the spatial and the temporal kernel by logistic regression we are making an average of the results of all trials, whereas when we fit the model we are taking into consideration the probability that the model makes the same choice as the original data for each trial and then summing the results. So, since the log-likelihood takes into account each trial, it is more informative than the kernel.

3.4.1 Combination of the different modules

To investigate the importance of the non linear transformation of the stimulus into evidence and the non linear accumulation of evidence, we used different modules combinations.

The stimulus to evidence module can either be a linear or logistic function, and it can either adapt throughout time or not. The decision-making module can either be linear (and behave as a perfect integrator) or non-linear (and behave like the double-well model). So we have eight possible combinations:

Name of the model	Stimulus to evidence module	Decision module
Perfect integrator with linear stimulus transformation	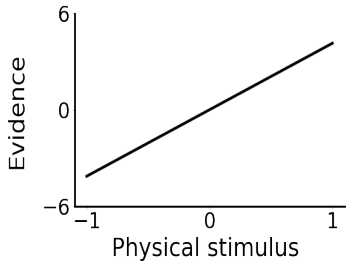	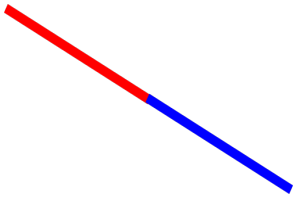
Perfect integrator with linear stimulus transformation and time adaptation	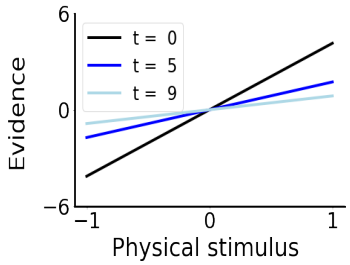	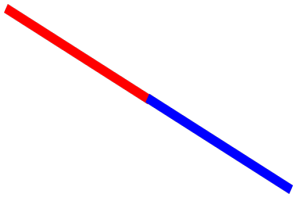
Perfect integrator with logistic stimulus transformation	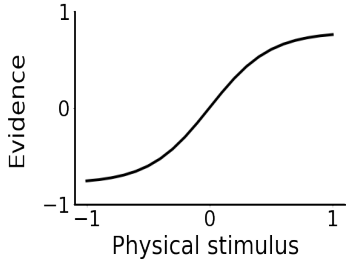	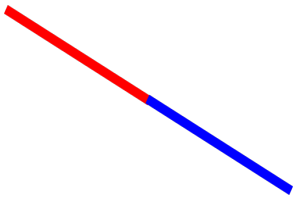
Perfect integrator with logistic stimulus transformation and time adaptation	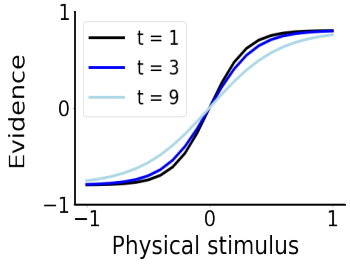	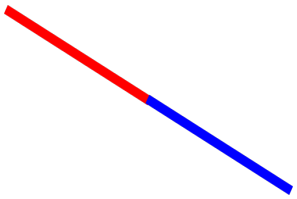

Double Well with linear stimulus transformation	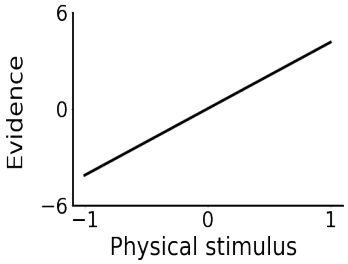	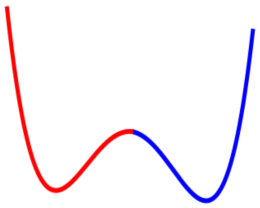
Double Well with linear stimulus transformation and time adaptation	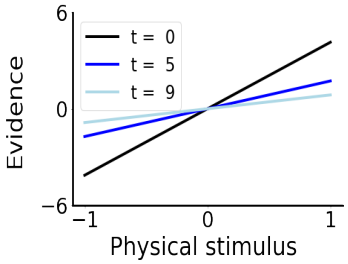	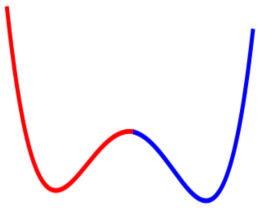
Double Well with logistic stimulus transformation	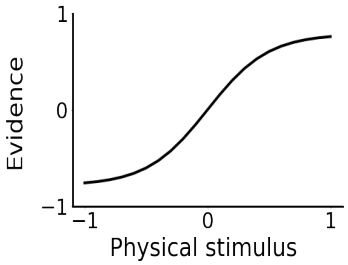	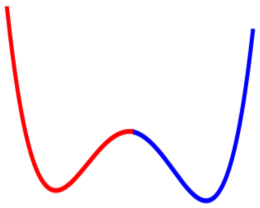
Double Well with logistic stimulus transformation and time adaptation	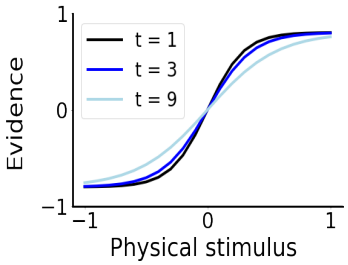	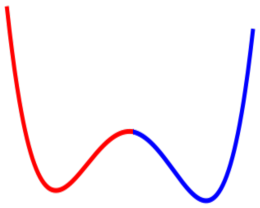

Table 3.1 – Eight possible combinations of the stimulus to evidence and decision module.

3.4.2 Model fitting

For each rat the data was fitted by each of the 8 possible combinations. The fit returned the parameters that maximize the likelihood. Then, the eight models were compared using the Akaike Information Criterion (eq. (3.3)), to determine which model

explains best the behaviour of each rat.

The model that explains best 3 of the 7 rats is the **double-well model with logistic stimulus transformation**. The results of the fits (fig. 3.8 and 3.9) show that this model is able to perfectly predict the psychometric curves without bias (fig. 3.9 a and g), and that it makes a fairly accurate prediction of the shape of the temporal (fig. 3.9 b, d and h) and spatial (fig. 3.9 c,e and i) psychophysical kernels.

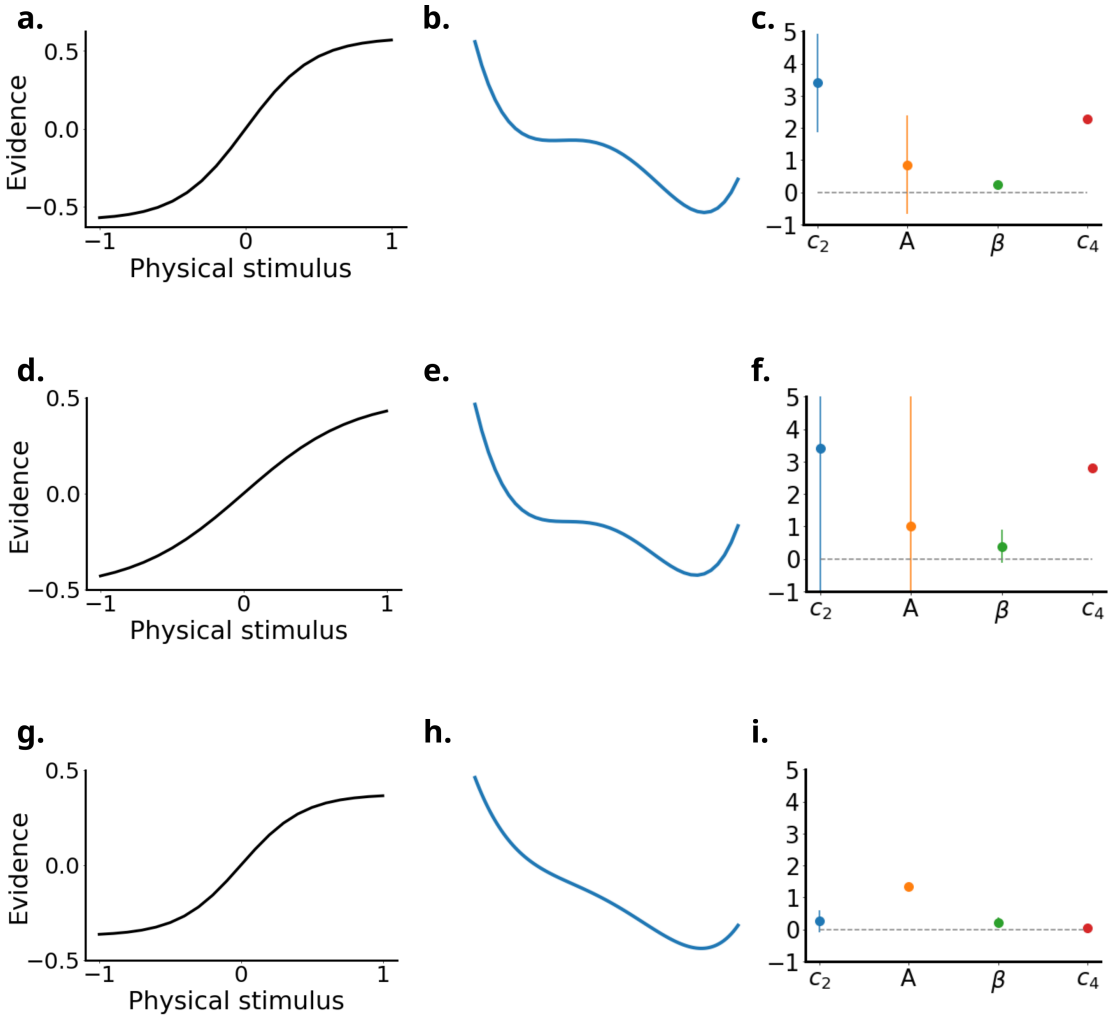

Figure 3.8 – **Characteristics of the fits of the double-well with logistic stimulus transformation.**

a. Rat 24 0.5 seconds: Logistic stimulus to evidence transformation. **b.** Rat 24 0.5 seconds: DW potential in the decision module. **c.** Rat 24 0.5 seconds: Parameters obtained. **d.** Rat 25 0.5 seconds: Logistic stimulus to evidence transformation. **e.** Rat 25 0.5 seconds: DW potential in the decision module. **f.** Rat 25 0.5 seconds: Parameters obtained. **g.** Rat 35 1 second: Logistic stimulus to evidence transformation. **h.** Rat 35 1 second: DW potential in the decision module. **i.** Rat 35 1 second: Parameters obtained.

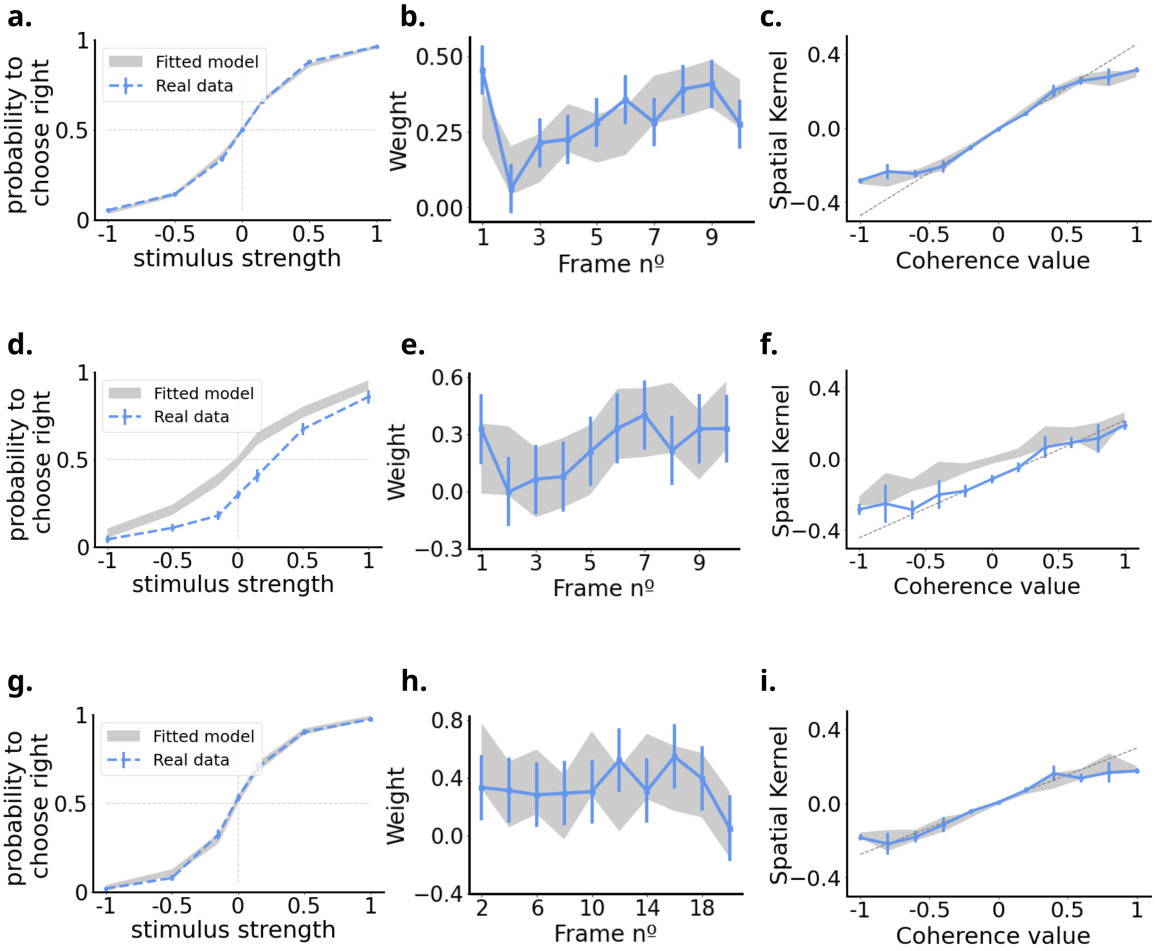

Figure 3.9 – Results of the fit for the double-well with logistic stimulus transformation. In blue, the experimental data, in grey the fitted model.

a. Rat 24 0.5 seconds: Psychometric curve. **b.** Rat 24 0.5 seconds: Temporal psychophysical kernel. **c.** Rat 24 0.5 seconds: Spatial psychophysical kernel. **d.** Rat 25 0.5 seconds: Psychometric curve. **e.** Rat 25 0.5 seconds: Temporal psychophysical kernel. **f.** Rat 25 0.5 seconds: Spatial psychophysical kernel. **g.** Rat 35 1 second: Psychometric curve. **h.** Rat 35 1 second: Temporal psychophysical kernel. **i.** Rat 35 1 second: Spatial psychophysical kernel.

For two of the rats, the best model was the **double-well model with logistic stimulus transformation which adapts throughout time**. The results of the fits (fig. 3.10 and 3.11) show that this model is able to correctly predict the psychometric curves without any bias (fig. 3.11 a), and that it makes a fairly good prediction of the shape of the temporal (fig. 3.11 b, d) and spatial (fig. 3.11 c, e) psychophysical kernels.

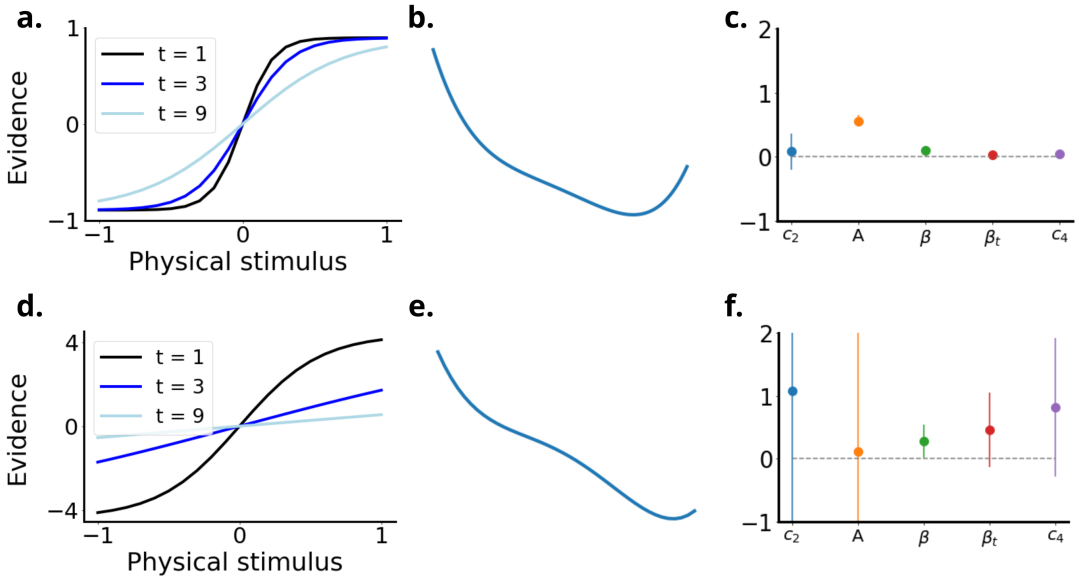

Figure 3.10 – Characteristics of the fits of the double-well with logistic stimulus transformation with time adaptation.

a. Rat 36 0.5 seconds: Logistic stimulus to evidence transformation with time adaptation. **b.** Rat 36 0.5 seconds: DW potential in the decision module. **c.** Rat 36 0.5 seconds: Parameters obtained. **d.** Rat 37 0.5 seconds: Logistic stimulus to evidence transformation with time adaptation. **e.** Rat 37 0.5 seconds: DW potential in the decision module. **f.** Rat 37 0.5 seconds: Parameters obtained.

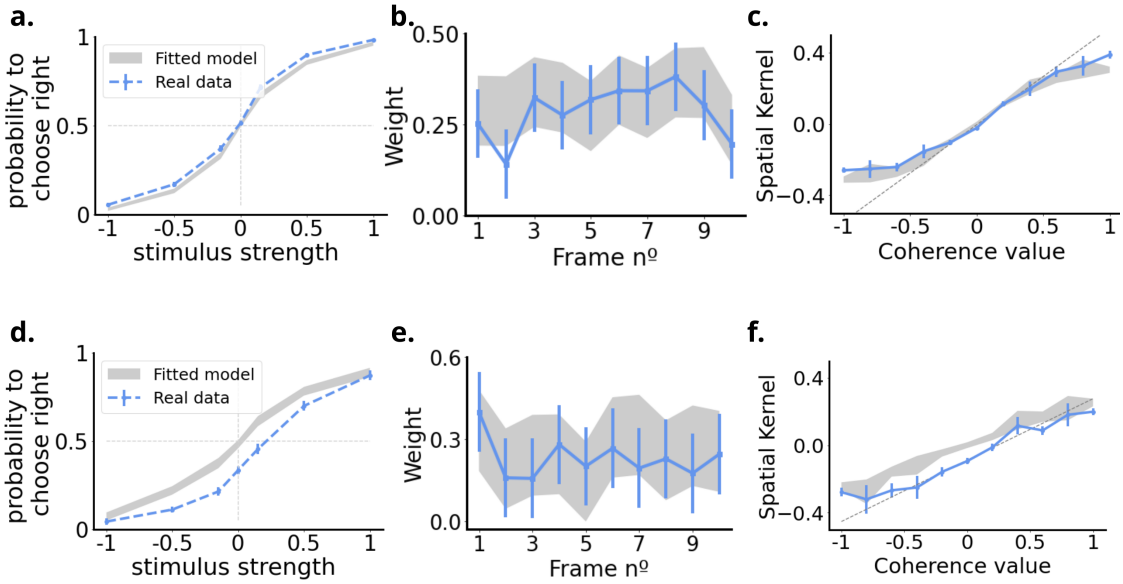

Figure 3.11 – Results of the fit for the double-well with logistic stimulus transformation. In blue, the experimental data, in grey the fitted model with time adaptation.

a. Rat 36 0.5 seconds: Psychometric curve. **b.** Rat 36 0.5 seconds: Temporal psychophysical kernel. **c.** Rat 36 0.5 seconds: Spatial psychophysical kernel. **d.** Rat 37 0.5 seconds: Psychometric curve. **e.** Rat 37 0.5 seconds: Temporal psychophysical kernel. **f.** Rat 37 0.5 seconds: Spatial psychophysical kernel.

Only one of the rats was better explained by a linear sensory module, and the best model for this rat was the **double-well model with linear stimulus transformation which adapts throughout time**. The results of the fits in this case (fig. 3.12 and 3.13) show that this model is able to correctly predict the psychometric curves, the temporal and the spatial psychophysical kernels of this rat.

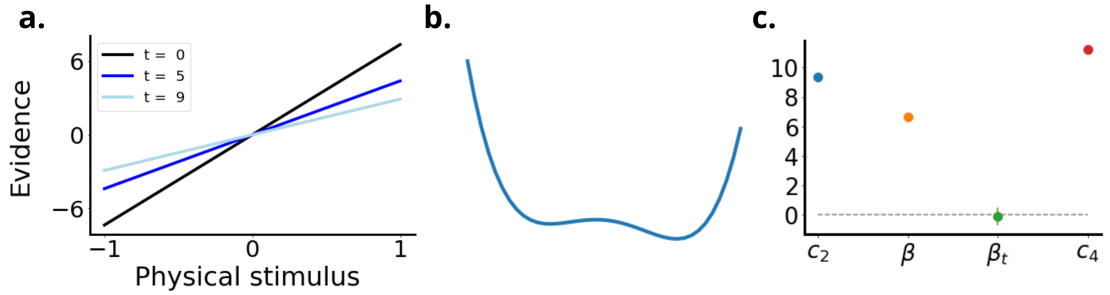

Figure 3.12 – Characteristics of the double-well model with linear stimulus transformation which adapts throughout time, which fits best rat 25 with a stimulus duration of 1 seconds.

a. Linear stimulus to evidence transformation which changes throughout time. **b.** Double-Well potential for the decision module. **c.** Parameters obtained in the fitting.

The results of the fit can be seen in figure 3.13. The model does a very good fit of the temporal and spatial psychophysical kernels, and the psychometric curve.

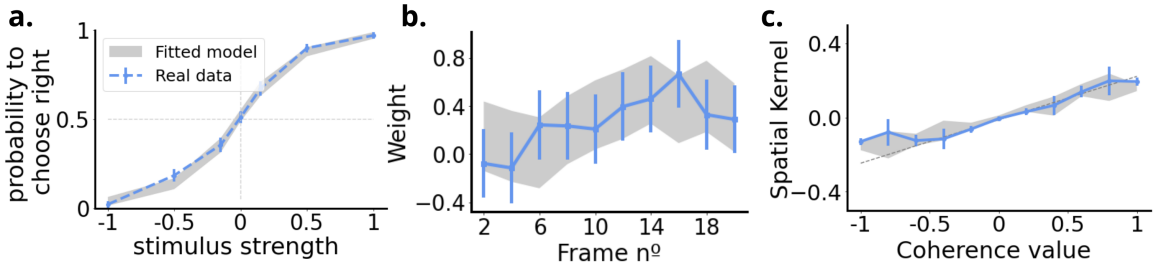

Figure 3.13 – Results of the fit for the double-well model with linear stimulus transformation which adapts throughout time, which fits best rat 25 with a stimulus duration of 1 seconds.

a. Psychometric curve, in blue the real data, in grey the model's prediction. **b.** Temporal Psychophysical kernel, in blue the real data, in grey the model's prediction. **c.** Spatial Psychophysical Kernel, in blue the real data, in grey the model's prediction.

There is only one rat which is better explained with a linear decision module, the best model for this rat is the **perfect integrator model with logistic stimulus transformation which adapts throughout time**. The results of the fits in this case

(fig. 3.14 and 3.15) show that the psychometric curve is not well predicted, due to the bias that this rat presents. The temporal psychophysical kernel does not show results as good as the previous fits, and the spatial psychophysical kernel is predicted well.

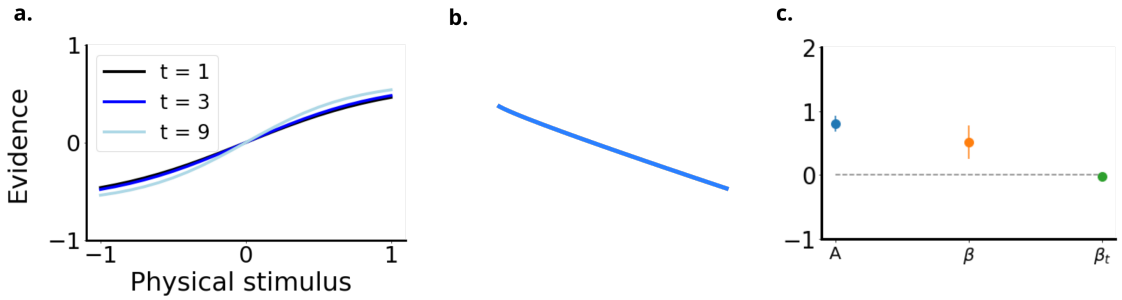

Figure 3.14 – Characteristics of the perfect integrator model with logistic stimulus transformation which adapts throughout time, which fits best rat 37 with a stimulus duration of 1 seconds.

a. Logistic stimulus to evidence transformation which changes throughout time. **b.** Linear (perfect integrator) for the decision module. **c.** Parameters obtained in the fitting.

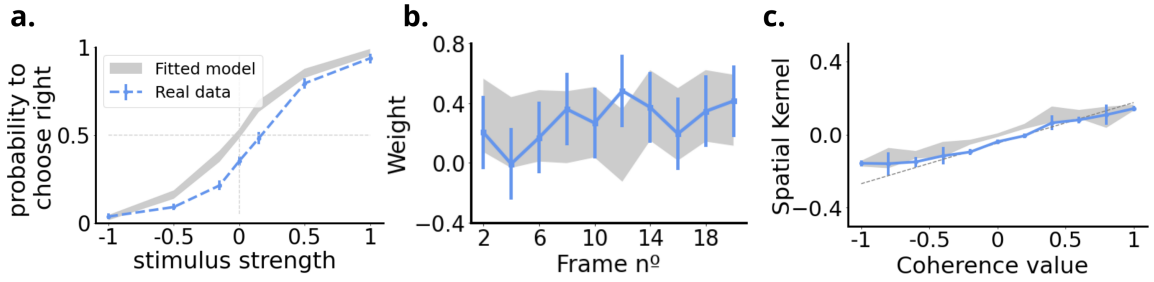

Figure 3.15 – Results of the perfect integrator model with logistic stimulus transformation which adapts throughout time, which fits best rat 37 with a stimulus duration of 1 seconds.

a. Psychometric curve, in blue the real data, in grey the model's prediction. **b.** Temporal Psychophysical kernel, in blue the real data, in grey the model's prediction. **c.** Spatial Psychophysical Kernel, in blue the real data, in grey the model's prediction.

We found that for the same rat but with different stimulus duration, the results of the fits varied considerably. In the case of rat 25, for a stimulus duration of 0.5 seconds the best model was the double-well model with logistic stimulus transformation, but for a stimulus duration of 0.5 seconds, it was the double-well model with linear stimulus transformation which adapts throughout time. In the case of rat 37, for a stimulus duration of 0.5 seconds the best model was the double-well model with logistic stimulus transformation which adapts through time, while for a stimulus duration of 1 second it was the perfect integrator with logistic stimulus transformation which adapts throughout time. Further study should be carried out in order to understand why rats seem to have

different model parameters for different stimulus durations, but this is not in the scope of this project.

3.4.3 Model comparison

To find which of the non-linearities of each module was more relevant to explain the psychophysical data, we compared the model which explains the experimental data better for each of the rats with and without the parameter that we wanted to test.

This was done by using the Akaike Information Criterion, which takes into account the likelihood of the fitting and the number parameters of the models in order to determine the quality of a model in comparison to the other ones. If the difference in AIC was greater than 10, we considered that there was strong evidence for this parameter (see Methods).

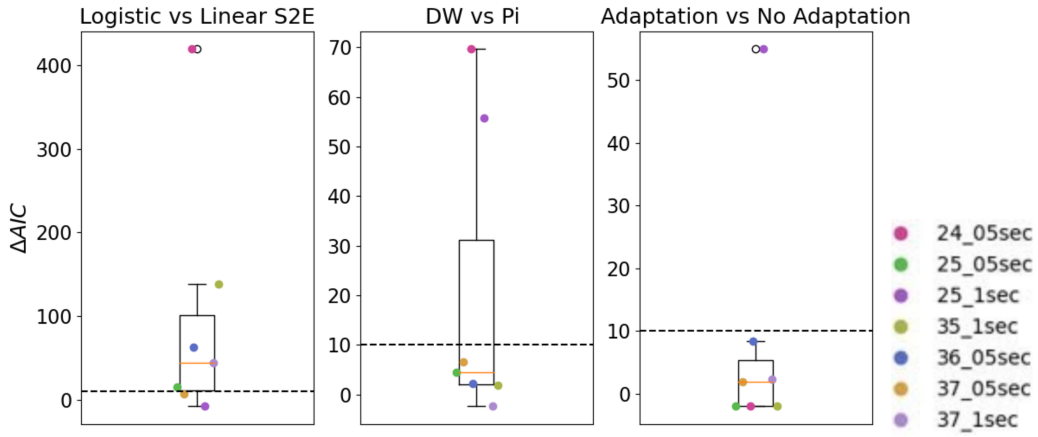

Figure 3.16 – Difference of AIC for the models with and without the parameters that we want to test.

Left: Logistic stimulus to evidence transformation. **Center:** Double-Well potential in the decision module. **Right:** Time adaptation of the stimulus to evidence module.

When we tested the logistic stimulus to evidence module compared to a linear one (fig. 3.16, left) we found that the non-linear transformation of this module was very relevant to explain the results of most of the rats. For one of the rats the result of the AIC comparison was -2. The model with a logistic stimulus to evidence transformation included the model with a linear transformation (i.e. choosing the correct parameter

the logistic function can approximate a linear function). Thus, in the case of linear transformation of evidence, the only difference between these models is the number of parameters (the model with a logistic stimulus to evidence module has one parameter more). Since the AIC penalizes 2 units for each additional parameter, the difference of AIC being -2 indicates that the logistic transformation is almost linear so both models are behaving exactly the same, which means that the logistic stimulus to evidence module does not seem to be relevant nor necessary to explain the experimental results of this rat. In contrast, one of the rats has an AIC difference between 0 and 1. In this case, this indicates that there is not strong evidence that this parameter is relevant to explain the data for this rat, but that the data is better explained by this model. When this happens, more trials should be included to have a more conclusive result.

The non-linearity on the decision module did not seem as relevant as the logistic stimulus to evidence module. In two of the rats, this characteristic was very relevant ($\triangle$AIC greater than fifty). But for 4 of the rats the result was between 0 and 10 indicating that there was not enough evidence for the double-well model. For one of the rats, the result of AIC difference was -2, which points that this rat was better explained with a linear (perfect integrator) decision module.

The time adaptation of the stimulus to evidence module was not important in almost all rats. In this case, only one of the rats had strong evidence that this module is relevant, and three of the rats had an uncertain conclusion (a difference of AIC ranging between 0 and 10). For three of the rats the result was -2 indicating that their results were better explained by a model without time adaptation.

4 | Execution Chronogram

This chapter contains the temporal distribution of the project, structured into tasks and sub-tasks that have a duration of approximately 300 hours, which has been performed between July 2020 and May 2021.

4.1 Work Breakdown Structure (WBS)

To achieve the objectives, this project can be divided into several tasks and sub-tasks (fig. 4.1).

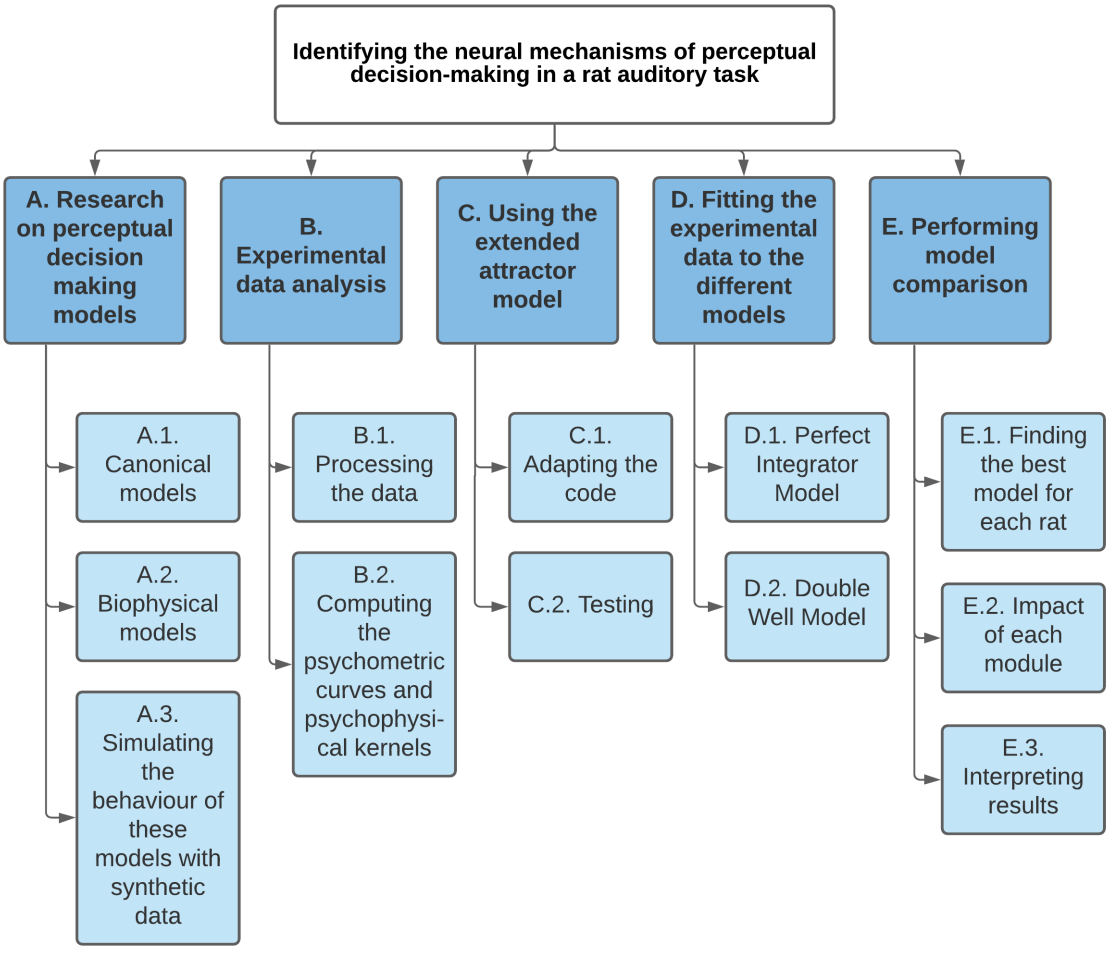

Figure 4.1 – Work Breakdown Structure of the project.

4.1.1 Work breakdown structure dictionary

Here, a description of what has been done in each of the tasks and sub-tasks in order to complete the project:

A. Research on perceptual decision-making models: Reading articles on both canonical and biophysical models to gather information, and using that information to simulate how these models work with synthetic data.

A.1. Canonical models: Gathering information on canonical models, DDMA, DDMR and PI.

A.2. Biophysical models: Gathering information on biophysical models, the double-well model.

A.3. Simulating the behaviour of these models with synthetic data: Programming with Python to understand the behaviour of both canonical and biophysical models. Understanding the effect that each parameter has on the results.

B. Experimental data analysis: Understanding the behaviour of the rats throughout the experiment.

B.1. Processing the data: Retrieving data, excluding non-valid trials and early training stages. Finding when the behaviour of the rats starts to be consistent.

B.2. Computing the psychometric curves and psychophysical kernels: Basic analysis of the behaviour of the rats throughout the experiment. Computing the psychometric curves and PK for different stimulus noises, training stages and stimulus strengths.

C. Using the extended attractor model: Understanding how to use the code of the extended attractor model, adapting the code to the rat experimental task and testing if the modified code has a good performance.

C.1. Adapting the code: Programming with Julia Lang and adapting the code so it can be used to model the experimental task.

C.2. Testing: Testing the adapted code to see if it fits correctly with synthetic data.

D. Fitting the experimental data to the different models: Using the adapted code to fit the experimental data with both the perfect integrator and the double-well model.

D.1. Perfect Integrator model: Fitting the experimental data using the perfect integrator with different variations of the stimulus to evidence transformation.

D.2. Double-well model: Fitting the experimental data using the double-well model with different variations of the stimulus to evidence transformation.

E. Performing model comparison: Comparing the models in order to find the relevance of each module.

E.1. Finding the best model for each rat: Computing the Akaike Information Criterion for each of the fits in order to see which is the model which does a better fit.

E.2. Impact of each module: Comparing the models with and without each mechanism to see the impact of each module.

E.3. Interpreting results: Understanding the biological meaning of these results.

4.2 Program Evaluation and Review Technique (PERT)

In order to determine the time for each of the tasks explained above, the PERT time, the optimistic time, the most likely time and the pessimistic time of each task was estimated, and the PERT time was obtained following the equation:

$$T_{PERT} = \frac{T_{opt} + 4T_{likely} + T_{pes}}{6} \tag{4.1}$$

If we sum the hours of each main activity of table 4.1, we obtain that the total time of the project is 297 hours (table 4.1), which will take place from July 2020 to May 2021.

	ID	Optimistic time (hours)	Most likely time (hours)	Pessimistic time (hours)	Time PERT (hours)
Research on perceptual decision-making models	**A**	**50**	**60**	**80**	**61,67**
Canonical models	A.1.	5	7	10	7,17
Biophysical models	A.2.	5	8	10	7,83
Simulating with synthetic data	A.3.	40	45	60	46,67
Experimental data analysis	**B**	**40**	**50**	**60**	**50**
Processing the data	B.1.	20	25	30	25
Computing the psychometric curves and PK	B.2.	20	25	30	25
Using the extended attractor model	**C**	**30**	**45**	**50**	**43,33**
Adapting the code	C.1.	20	28	30	27
Test	C.2.	10	17	20	16,33
Fitting the experimental data	**D**	**70**	**100**	**140**	**101,67**
Perfect Integrator Model	D.1.	30	40	60	41,67
Double-well Model	D.2.	40	60	80	60
Performing model comparison	**E**	**20**	**40**	**60**	**40**
Finding the best model for each rat	E.1.	10	20	25	19,17
Impact of each module	E.2.	5	10	15	10
Interpreting results	E.3.	5	10	20	10,83

Table 4.1 – **PERT time for all the tasks.** In bold, the main tasks of the project.

Then a sequence matrix was created to know which tasks precede other task (table 4.2):

Predecessor activity	Activity	Following activity
-	A	B, C
A	B	D
A	C	D
B, C	D	E
D	E	-

Table 4.2 – Task sequence matrix.

Using this sequence matrix a PERT diagram was created (fig. 4.2) taking into account the PERT time calculated before, obtaining the critical path of the activities to be followed. The critical part is colored in blue and it can be observed that the only activity which is not included in the critical path is activity B (experimental data analysis).

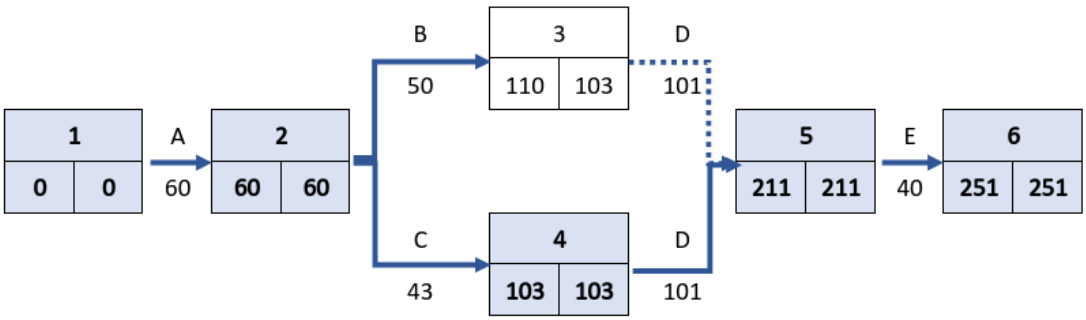

Figure 4.2 – PERT diagram. In blue, the critical path of the project.

4.3 Gantt Diagram

Our project started in July 2020 and ended in May 2021, having a duration of 11 months. The project was divided into a set of tasks (table 4.1) which have been distributed through the eleven months. In the Gantt chart (fig. 4.3), we reflected the original timing of the tasks. These timings were successfully followed and they contributed to the correct development of the project.

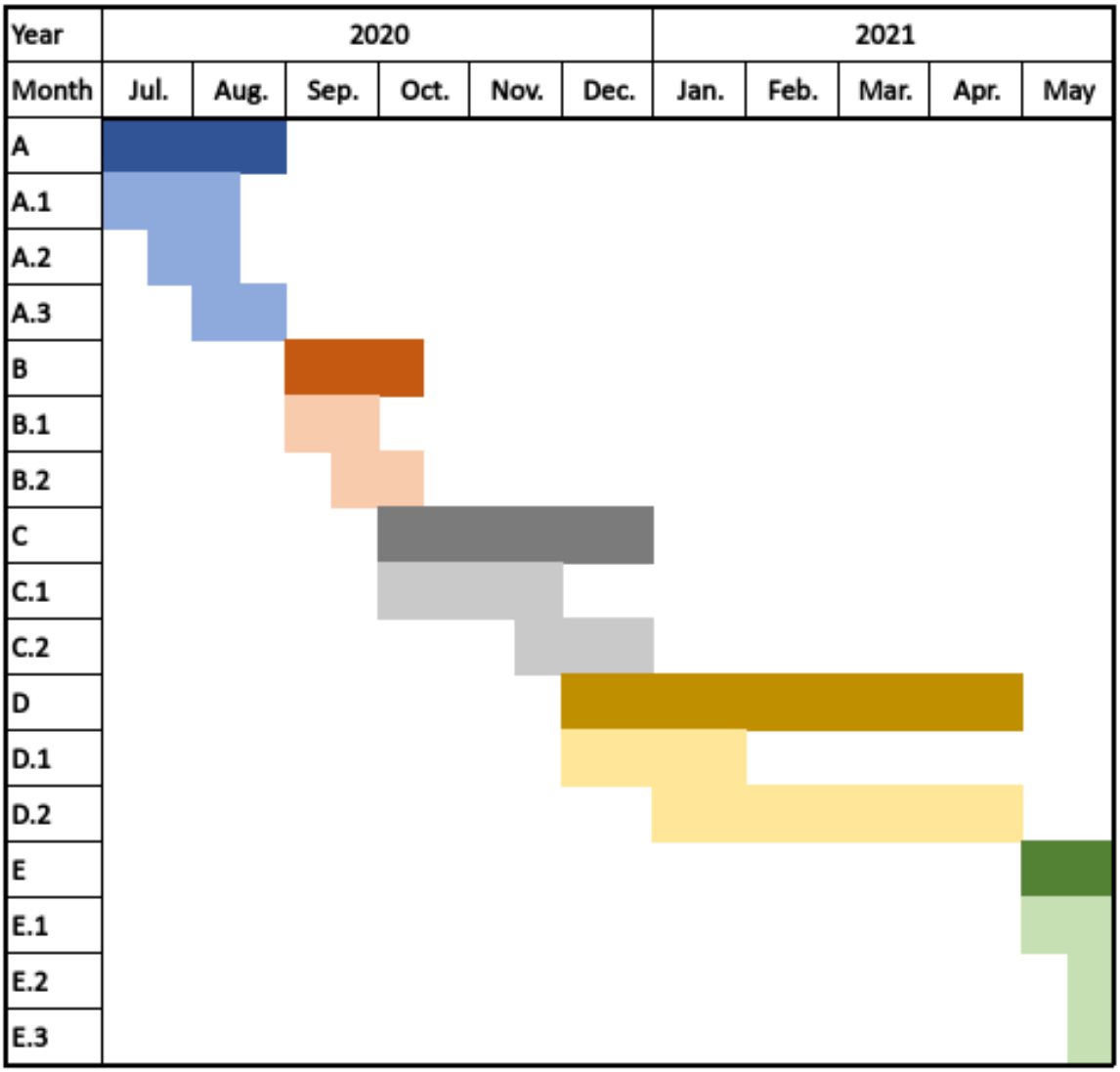

Figure 4.3 – Gantt diagram of the project.

Project tasks over time represented in a Gantt diagram. Time is divided by months and tasks which include several tasks are colored darker than individual tasks.

5 | Technical Viability

When starting a project it is useful to analyse which are the strengths, weaknesses, opportunities and threats that it is submitted to. That is why a SWOT chart has been created (fig. 5.1).

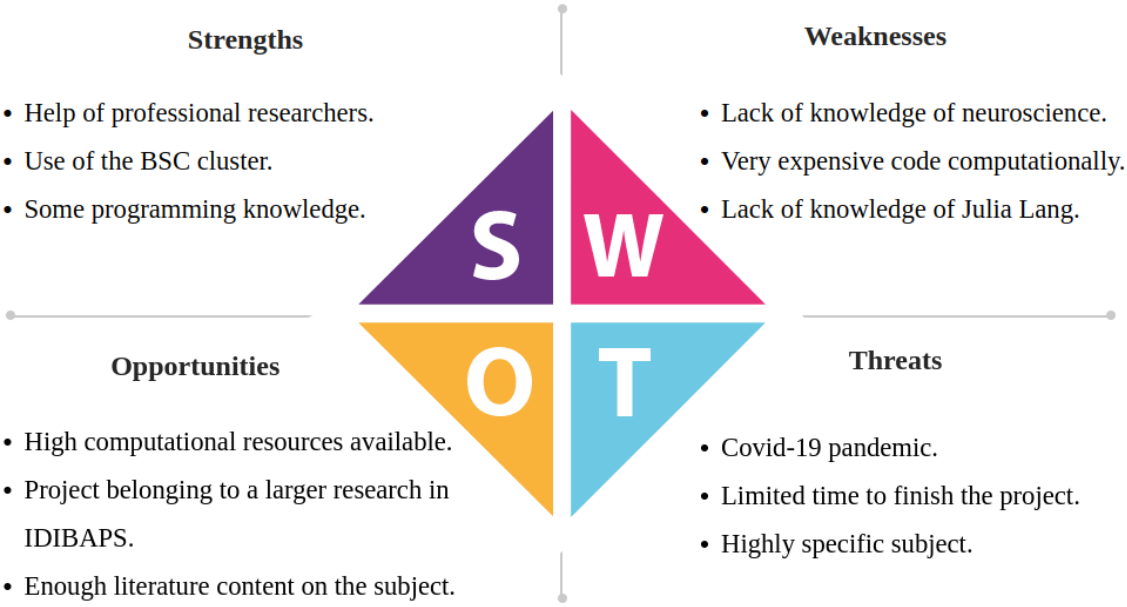

Figure 5.1 – **SWOT.** Strengths, weaknesses, opportunities and threats.

The **strengths** (internal factors) that this project has are that it will be done with the help of professional researchers from the IDIBAPS brain circuits and behaviour lab, and that resources such as the use of the cluster from the Barcelona Supercomputing Center will be available. Also, it has to be taken into account that this project will be done based on programming language knowledge which has been acquired throughout the degree.

The **opportunities** (external factors) that this project is submitted to are the high computational resources which are growing exponentially recently and the fact that the project is integrated in a larger research performed at IDIBAPS. It is also good that there is enough literature on the subject.

The **weaknesses** (internal factors) that this project is presented with are the lack of knowledge of neuroscience and perceptual decision-making, since very little has been

studied during the degree. It has to be taken into consideration that the code used is very expensive computationally, so the time will be limited by the computational power needed. Also, a programming language (Julia Lang) which I had not used had to be learned in order to use and modify the code.

The **threats** (external factors) that apply to this project are the Covid-19 pandemic, which limits the interaction with the director and tutor of the project, the limited timeline in which the project has to be carried out and the highly specific subject of study.

6 | Conclusions and future directions

6.1 Conclusions

The purpose of this project was to understand how rats receive and integrate the information to make a categorical choice. To this aim, we characterized the behaviour of the rats with their psychometric curves and the spatial and temporal kernels. To further analyse the importance of the different neural mechanisms, we built a new extended attractor model that can fit the psychophysical data. By fitting this model, we have shown that the brain does not transform linearly the stimulus into evidence and that, at least for a subset of rats, the accumulation of evidence is not perfect. We have also shown that adaptation is not an important mechanism in our tasks.

Throughout the project, we analyzed the impact of every frame and the impact of each stimulus strength on the final response. The results of the temporal psychophysical kernels show that most of the rats had neither a recency nor a primacy pattern, but a mixture of both, while the results of the spatial psychophysical kernels indicate that all of the rats are underweighting extreme stimulus evidence.

Taking into account these results, it is clear that the temporal and spatial psychophysical kernels cannot be created by canonical models of decision-making. This means that there has to be a non-linear pattern in either the stimulus to evidence, the decision module or both. It cannot be determined in which of the modules this non-linearity is located just by looking qualitatively at the experimental result, this is why we fitted an extended attractor model, obtaining a quantitative result which allowed us to identify the underlying mechanisms that explain the behaviour of the rats.

This extended attractor model was composed of two modules: the stimulus to evidence module and the decision module. The stimulus to evidence module has not been taken into account in other studies (Kiani et al. (2008), Drugowitsch et al. (2016)) even though the spatial psychophysical kernels underweight extreme evidence, but in this project we have shown that the non-linearity of this module is very relevant to explain the behaviour of most of the rats.

A novelty in our project is that we have been able to fit a neurobiological model, obtaining results that can be interpreted in neurological networks. For most of the rats, the double-well model is better than a perfect integration, but we only found strong evidence for 2 of the rats. Future experiments with more subjects (animals or humans) and more trials for subjects should be able to assess if rats and humans can perfectly accumulate evidence (Brunton et al. (2013)) or if the non-linear potential plays an important role in the decision process (Prat-Ortega et al. (2021), Roxin and Ledberg (2008), Keung et al. (2020)).

The time adaptation of the stimulus to evidence transformation module did not seem to be relevant in most of the rats, even though in other studies it seems to have an important impact (Yates et al. (2017)). This result should be compared with other tasks, because it could be happening due to the nature of the experimental task we used. One of the possible causes would be the duration of the stimuli which is very short (0.5 or 1 second). Another possibility is that the type of stimuli used (in our case auditory) does not present this time adaptation, in other studies with other tasks (such as motion) it seems to be very relevant.

In the results section, we have shown that the rats have learned the task correctly because their accuracy decreased with task difficulty. But in experiments, subjects or animals may be biased towards one of the choices by different mechanisms (Urai et al. (2019)). In our case the bias could be located on the initial condition, on the potential of the diffusion process or on the logistic function on the stimulus to evidence module. By making a qualitative assessment of the psychometric curve, it is not possible to differentiate which of these biases is causing the shift in the results of some of the rats, so further studies adding the bias parameter to the model should be performed to understand which of these parameters is generating this behaviour.

To summarize, our work shows that model fitting is a useful tool to investigate different brain mechanisms and that nonlinear dynamics could be important not only during evidence accumulation but also during the transformation of stimuli into evidence.

6.2 Limitations and future perspectives

The main limitations encountered throughout the project were the time constraint and the amount of trials and subjects in the experimental data.

If the project were to be repeated with more trials for each of the rats, and some rats were added to the study, the results would be more conclusive. Also, regarding the timeline of the project, there are several tasks which remain pending to do in future advances:

- Adding biases as parameters to the model, to see which kind of bias is affecting the behaviour of the rats.
- Adapting the code to fit together trials of 0.5 and 1 second duration of stimulus (in order to fit those rats which have both stimulus durations).
- Checking if the results are similar for other tasks and other species (such as humans or monkeys) to see if the results are general. Another study is being carried out at IDIBAPS in which the same model is being fitted using human data performing a visual task, and results seem to indicate that the logistic transformation of the stimulus into evidence and the double-well in the decision module are very important to explain the psychophysical results.
- Adding an urgency signal to the potential of the double-well (adaptation through time of the shape of the potential).

Bibliography

Britten, K. H., Shadlen, M. N., Newsome, W. T., and Movshon, J. A. (1992). The analysis of visual motion: A comparison of neuronal and psychophysical performance. *Journal of Neuroscience*, 12(12):4745–4765.

Brunton, B. W., Botvinick, M. M., and Brody, C. D. (2013). Rats and humans can optimally accumulate evidence for decision-making. *Science*, 340(6128):95–98.

Butts, D. A. and Goldman, M. S. (2006). Tuning curves, neuronal variability, and sensory coding. *PLoS Biology*, 4(4):639–646.

Drugowitsch, J., Wyart, V., Devauchelle, A. D., and Koechlin, E. (2016). Computational Precision of Mental Inference as Critical Source of Human Choice Suboptimality. *Neuron*, 92(6):1398–1411.

Gold, J. I., Law, C. T., Connolly, P., and Bennur, S. (2008). The relative influences of priors and sensory evidence on an oculomotor decision variable during perceptual learning. *Journal of Neurophysiology*, 100(5):2653–2668.

Keung, W., Hagen, T. A., and Wilson, R. C. (2020). A divisive model of evidence accumulation explains uneven weighting of evidence over time. *Nature Communications*, 11(1):1–9.

Kiani, R., Cueva, C. J., Reppas, J. B., and Newsome, W. T. (2014). Dynamics of neural population responses in prefrontal cortex indicate changes of mind on single trials. *Current Biology*, 24(13):1542–1547.

Kiani, R., Hanks, T. D., and Shadlen, M. N. (2008). Bounded integration in parietal cortex underlies decisions even when viewing duration is dictated by the environment. *Journal of Neuroscience*, 28(12):3017–3029.

Mulder, M. J., Wagenmakers, E. J., Ratcliff, R., Boekel, W., and Forstmann, B. U. (2012). Bias in the brain: A diffusion model analysis of prior probability and potential payoff. *Journal of Neuroscience*, 32(7):2335–2343.

Nienborg, H. and Cumming, B. G. (2009). Decision-related activity in sensory neurons reflects more than a neurons causal effect. *Nature*, 459(7243):89–92.

Prat Ortega, G. (2019). *Attractor dynamics in perceptual decision making: from theoretical predictions to psychophysical experiments*. PhD thesis, Universitat Autònoma de Barcelona.

Prat-Ortega, G., Wimmer, K., Roxin, A., and de la Rocha, J. (2021). Flexible categorization in perceptual decision making. *Nature Communications*, 12(1):1–47.

Resulaj, A., Kiani, R., Wolpert, D. M., and Shadlen, M. N. (2009). Changes of mind in decision-making. *Nature*, 461(7261):263–266.

Roitman, J. D. and Shadlen, M. N. (2002). Response of neurons in the lateral intraparietal area during a combined visual discrimination reaction time task. *Journal of Neuroscience*, 22(21):9475–9489.

Roxin, A. and Ledberg, A. (2008). Neurobiological models of two-choice decision making can be reduced to a one-dimensional nonlinear diffusion equation. *PLoS Computational Biology*, 4(3):1000046.

Shadlen, M. N. and Newsome, W. T. (2001). Neural basis of a perceptual decision in the parietal cortex (area LIP) of the rhesus monkey. *Journal of Neurophysiology*, 86(4):1916–1936.

Shen, S. and Ma, W. J. (2018). Variable Precision in Visual Perception. *Psychological Review*.

Urai, A. E., De Gee, J. W., Tsetsos, K., and Donner, T. H. (2019). Choice history biases subsequent evidence accumulation. *eLife*, 8.

Wang, X.-J. (2002). Probabilistic decision making by slow reverberation in cortical circuits. *Neuron*, 36:955–968.

Waskom, M. L. and Kiani, R. (2018). Decision Making through Integration of Sensory Evidence at Prolonged Timescales. *Current Biology*, 28:3850–3856.e9.

Yartsev, M. M., Hanks, T. D., Yoon, A. M., and Brody, C. D. (2018). Causal contribution and dynamical encoding in the striatum during evidence accumulation. *eLife*, 7.

Yates, J. L., Park, I. M., Katz, L. N., Pillow, J. W., and Huk, A. C. (2017). Functional dissection of signal and noise in MT and LIP during decision-making. *Nature Neuroscience*, 20(9):1285–1292.